AD-774 701

HIGH ENERGY LASER WINDOWS

R. W. Rice

Naval Research Laboratory

Prepared for:

Advanced Research Projects Agency

31 December 1973

ARPA Order
2031

AD 774 701

Program Code
3D10

Principal Investigator:
R. W. Rice
(202)767-2131

Contractor:
U. S. Naval Research Laboratory

Effective Date of Contract:
1 July 1973

Contract Expiration Date:
30 June 1974

Amount of Contract:
$225K

The views and conclusions contained in this document are those of the authors and should not be interpreted as necessarily representing the official policies, either expressed or implied, of the Advanced Research Projects Agency or the U. S. Government.

84

Forward

This semi-annual technical report summarizes work performed by personnel of the U. S. Naval Research Laboratory, Washington, D.C. 20375, under ARPA Order 2031. The program was coordinated by Mr. R. Rice and Dr. P. Becher and monitored by Dr. C. M. Stickley of ARPA. The report covers the period 1 July 1973 through 31 December 1973.

This reports consists primarily of the NRL papers presented at the Third Annual High Power Infrared Laser Window Materials Conference in November 1973 at Hyannis, Mass. Some of this information thus overlaps with the previous report. This is supplemented with recent material on mechanical behavior. The list of publications and presentations at the beginning of the report illustrate several of the major results of this program.

Recent Publications and Presentations

1. J. A. Harrington and M. Hass, "Temperature Dependence of Multiphonon Absorption," Phys. Rev. Letters 31, 710 (1973).

2. J. W. Davisson, "Surface Finishing of Alkali Halides," J. Appl. Phys. (submitted).

3. M. Hass, J. W. Davisson, P. H. Klein, and L. Boyer, "Infrared Absorption in Low Loss KCl Single Crystals Near 10.6μm," J. Appl. Phys. (submitted).

4. H. B. Rosenstock, "Multiphonon Absorption by Ionic Crystals: Temperature Dependence," J. Appl. Phys. 44, 4473 (1973).

5. H. B. Rosenstock, "Multiphonon Absorption in Alkali Halides: Quantum Treatment of Morse Potential," Phys. Rev. B (accepted for publication).

6. P. F. Becher and R. W. Rice, "Strengthening Effects in Press Forged KCl," J. Appl. Phys. 44, 2915 (1973).

7. J. A. Harrington, L. Boyer, and M. Hass, "Multiphonon Absorption in Alkali Halides Near 10.6μm," Amer. Phys. Soc., Philadelphia, Pa., March 1974.

8. H. B. Rosenstock and L. L. Boyer, "Theory of Multiphonon Absorption," Amer. Phys. Soc., Philadelphia, Pa., March 1974.

9. P. F. Becher, R. W. Rice, P. H. Klein and S. W. Freiman, "Mechanical Properties of Press Forged Halide Laser Windows: Grain Size and Alloying Dependence," Am. Ceram. Soc., Cincinnati, Ohio, May 1973.

TABLE OF CONTENTS

1.0 INTRODUCTION AND SUMMARY

The goal of this program is to reduce the absorption, and improve the mechanical properties, of alkali halides for laser window use. Very low absorption has resulted from improved crystal growth and finishing of KCl. The mechanisms of absorption are being studied both theoretically and experimentally as a guide to further reducing absorption. With KCl as a model material, higher yield strengths and fracture toughness have been achieved by forging crystals to obtain fine grained polycrystalline bodies supplemented by alloying or irradiation.

During this reporting period, a number of important results in infrared absorption have been achieved:

1. Nearly intrinsic bulk absorption has been found at 10.6μm in chemically polished KCl crystals which were grown in a reactive atmosphere.

2. Intrinsic and extrinsic absorption in KCl has been distinguished by studies of its temperature dependence.

3. A 9.8μm surface impurity band in KCl has been detected by laser calorimetry.

4. Frequency and temperature dependence of absorption at wavelengths <10.6μm has been studied with the spectral emittance studies at NELC.

Studies of mechanical properties of KCl have shown that:

1. Polycrystalline yield strengths have been raised as high as 7500 psi in forgings of KCl-$SrCl_2$ crystals in which 20 ppma of strontium was incorporated during RAP Bridgman crystal growth.

2. Fracture energy increases with yield stress; values up to 3 J/m^2 are obtained by a combination of alloying and press forging.

3. Residual forging strains can be retained in alloyed forgings and affect strength, but these can be removed by annealing, leaving yield strengths of ~6000 psi.

4. Annealing of alloyed forgings is possible because of their enhanced microstructural stability (e.g., limited or no grain growth with anneals up to 450°C).

Work will continue toward our goals, reducing absorption and improving mechanical properties, by determining the mechanisms involved. Because of the success in growth of very low loss $SrCl_2$ alloyed KCl, the need for using less hygroscopic $BaCl_2$ alloying is being re-evaluated. Growth-purification mechanisms and alloy content-forging-annealing interactions will be further refined for optimum mechanical and optical behavior. The mechanisms of crack growth and the importance of fracture energy in controlling window failure will be further evaluated, including additional laser testing. Because of the microstructural stability achieved by annealing and alloying, long-term tests of stability will be limited. Absorption studies, including improved calorimetry and emittance techniques for low loss materials will compare theory and experimental data over a wide range of wavelengths. Increased attention will be given to absorption in strengthened materials as a function of length, frequency, and temperature, with some emphasis in the 3-5μm region.

STRENGTHENING BEHAVIOR IN POLYCRYSTALLINE KCl

P. F. Becher, S. W. Freiman, P. H. Klein and R. W. Rice
Naval Research Laboratory
Washington, D. C. 20375

Abstract

Further strengthening of polycrystalline KCl beyond ≈4500 psi by reducing grain size substantially below 5μm is not practical. Since the single crystal yield stress of KCl increased ≈threefold with the addition of only 20 ppma Sr^{+2}, Sr^{+2}-doped KCl was selected as a model for press forged divalent alloys. Yield strengths as high as 7500 psi were achieved in the resultant polycrystalline KCl-<25 ppma Sr^{+2} bodies. The supplemental solution strengthening achieved in Sr^{+2} doped polycrystalline KCl was accompanied by strain hardening effects and was thus altered by forging and annealing temperatures. Furthermore, Sr^{+2} additions retarded recrystallization during forging, as well as recovery and grain growth during annealing (e.g., fully recrystallized microstructures were stable when annealed at 450°C).

The fracture energy of KCl crystals (0.2 J/m^2) improved with increasing yield stress obtained by either Sr^{+2} additions or γ-irradiation ($\gamma_f \leq 1$ J/m^2). Polycrystalline forgings had fracture energies >2 J/m^2, ~tenfold greater than their parent crystals. The low infrared absorption achieved in Sr^{+2} doped and pure KCl crystals and subsequent pure KCl forgings further accentuated the improvement which can be achieved in the alkali halides.

1. INTRODUCTION

Previously, Becher and Rice (1972) showed that polycrystalline KCl formed by press forging single crystals has significantly (up to twenty-fold) greater yield strength than the starting crystals. The Petch type grain size dependence of yield stress confirms strengthening is by grain boundary resistance to slip, but yield strengths are limited to ≤5000 psi because of practical difficulties in producing grain sizes much less than 5μm. Since higher yield strengths are desirable, additional strengthening mechanisms were sought. Divalent solid solution alloying, with Sr^{+2} as a model, was selected since Chin et al (1973) found very small additions give substantial strengthening. The study was also stimulated by the fact that the Sr^{+2} doped KCl crystals grown in the NRL program had extremely low absorption coefficients (Klein, 1973). This paper discusses the influence of Sr^{+2} on yield of and fracture energy of single crystal and polycrystalline KCl, as well as on the forging behavior of KCl.

2. EXPERIMENTAL

The experimental techniques and materials are fully described in previous reports (Becher and Freiman (1972), Becher and Rice (1972 and 1973c)) and thus are only briefly covered here. The Sr^{+2} doped crystals consisted of three <100> A crystals (1 cm^3)- Czochralski growths in argon using crushed KCl stock which was zone-refined in chlorine atmosphere, and six ≈ <111> B crystals (2.5 cm diameter x 3 cm high)- Bridgeman grown in Ar-CCl_4. B and A crystals exhibited total uncorrected absorption coefficients of $<3x10^{-4}cm^{-1}$ and $\leq 1x10^{-2}cm^{-1}$, respectively. Strontium contents of

the as grown B crystals were measured* and found to be ≈1/3 of the amount added to the Bridgeman charge. The size limitation of the A crystals precluded analysis so only as added contents are reported, but a similar ratio of as-grown to as-added strontium content might be expected.

Test specimens were shaped by cleaving or cutting (alumina grit, rubber bonded cut off wheel, isopropanol coolant), followed by water polishing on cloth; then a polish in a flowing water bath and an ethanol rinse, and drying in warm air. Mechanical tests at 23°C, ≈50% RH consisted of 3 point bend tests at a tensile surface strain rate of $5 \times 10^{-6} s^{-1}$ for yield strength (proportional limit) determination and a modified double cantilever beam test (Freiman et al (1972)) for fracture energy studies. Specimen treatments also included annealing at various temperatures (50° to 450°C) for 3/2 h in an externally heated 99.9% alumina tube with a flowing argon atmosphere. The effects of annealing on yield strength were conducted with as grown crystals, as forged bodies and crystals which were prestrained in bending to 0.2% tensile surface plastic strain. The annealed prestrained crystals were subsequently tested keeping the tensile surface and area of maximum strain the same as that in the prestraining procedure.

Press forging was conducted at a fixed crosshead speed (initial $\dot{\epsilon} = 5 \times 10^{-2} m^{-1}$), generally with copper constraining sleeves. A silicone fluid was used to lubricate the end and sleeve faces. The Sr^{+2} doped KCl crystals were forged in the temperature range of 175°C to 300°C while flushing the forging chamber with helium.

*Mass spectroscopy and atomic absorption analyses kindly performed at the Naval Research Laboratory by Mr. J. G. Allard and Dr. P. E. R. Nordquist, respectively.

"Normal" crystal forgings were deformed to a desired height reduction at 180° to 260°C, then ejected into an annealing furnace and held for 1/2 hr. at 125°C, followed by cooling to 23°C in 1/2 hr. These are distinguished from "high temperature-slow cooled" forgings (200 ppma Sr^{+2} A and ≥20 ppma Sr^{+2} B crystals) which were forged at >280°C and cooled directly to 23°C in 1-1/2 to 2 hrs.

3. RESULTS

The influence of Sr^{+2} on the press forging behavior and the resultant microstructure of KCl are presented, followed by the room temperature yield behavior of (1) KCl crystals which were solid solution hardened by Sr^{+2} and (2) polycrystalline KCl-$SrCl_2$. Finally, fracture energy experiments with KCl crystals and forgings are discussed.

3.1 Press Forging

The deformation behavior of pure and alloyed crystals to produce crack-free forgings at essentially a constant forging temperature (200° ± 15°C) is shown in Fig. 1. Comparison illustrates that strontium ion additions raise the observed yield stress of unconstrained forgings where the forging stress is uniaxial and increases the strain hardening rate during constrained (biaxial stress state) forging (Fig. 1). The stress-strain behavior of constrained forgings is dominated by flow of the copper sleeve, thus only the yield of unconstrained forgings exhibit the effects of Sr^{+2} additions. The copper constraining sleeve results in biaxial (axial and radial) forging stresses which by promoting multiple slip would enhance the strain hardening effects of Sr^{+2} additions.

Forgings of KCl-1000 ppma $SrCl_2$ A crystals clearly exhibit an increase in recrystallization temperature such that forging at 175°C results in a partially recrystallized structure, Fig. 2A. Note that fine grains developed in bands which intersect and surround large areas of ill- or undefined microstructure. These bands correspond to the expected <110> slip bands and suggest that grains nucleate within these slip bands, particularly at their intersections. Increasing the forging temperature results in more homogenous recrystallization, so that in the range of 225° to 260°C, a fully recrystallized structure occurs (Fig. 2b). This differs from pure KCl, which can recrystallize at 125°C under comparable forging conditions (Becher and Rice (1972 and 1973b)).

The forging temperatures of the low Sr^{+2} content (<20 ppma) B crystals were kept at 200° to 225°C to eliminate cracking and all were fully recrystallized, Fig. 2C. Thus, any changes in recrystallization temperature with these smaller strontium additions to B crystals are felt to occur at temperatures below 200°C.

3.2 Yield Behavior

3.2.1 SINGLE CRYSTALS

The A crystals with 200, 1000 and 5000 ppma $SrCl_2$ additions have resolved shear stresses of 640, 395, and 1050 psi, respectively. This inconsistent increase in strength with alloy additions to A crystals contrasts with the uniform increase observed in B crystals and may reflect large changes in strontium content with the crystal length, by Sr^{+2} rejection during growth of these smaller A crystals. The yield stress of B crystals follows a 1/2 power dependence of the actual strontium content, Fig. 3, consistent with previous studies

by Chin et al (1973) and Sibley et al (1973). During room temperature plastic flow, strain hardening rates were also greater in Sr^{+2} doped crystals.

Annealing studies of as-grown crystals, Fig. 4a, show that the yield stress of A crystals with 5000 ppma Sr^{+2} additions goes through a minimum in the range of 250°C to 400°C. This softening, also noted by Chin et al (1973), is associated with precipitation, as indicated by the clouding of samples annealed at 350°C. The gradual drop in strength for B crystals annealed above 300°C indicates that softening may also have been initiated. The prestrain studies, Fig. 4b, illustrate that with increase in strontium content, the temperature is raised at which the prestrain hardening effects on yield strength are recovered (relieved).

3.2.2 POLYCRYSTALLINE KCl

Analysis of the strengthening achieved in polycrystalline KCl by divalent cation additions is based on the Petch equation:

$$\sigma_y = \sigma_o + kd^{-1/2}$$

where σ_y is the polycrystalline yield strength, σ_o is the intercept value or lattice resistance to slip (≈ single crystal yield stress), k the slope, and d the average grain size. Strengthening by grain boundary resistance to slip is reflected in the term $kd^{-1/2}$, while alloying effects may show up in either σ_o or k.

Studies of A crystals (Becher and Rice (1973c)) indicate that the Petch slope is raised for large strontium additions (1000 ppma). This was attributed to increased grain boundary resistance to slip by chemically altered boundaries with increased strontium content. These preliminary results emphasized that further work was needed to clarify the situation.

Comparison of the Petch behavior of Sr^{+2} doped B forgings with pure forgings illustrate two strengthening effects with Sr^{+2} doping: Group I which parallels pure KCl and Group II with the higher slope, Fig. 5. Note that Group I bodies contain ≥20 ppma Sr^{+2} and are high-temperature, slow-cooled forgings, while Group II bodies contain <20 ppma Sr^{+2} and are normal forgings.

As the difference between Group I and II appears to be related to the forging temperatures used, their yield strength changes with annealing have been studied to observe if recovery of residual strains occurred. At the same time, grain growth temperatures (± 50°C) could be determined. These findings for Sr^{+2} doped B forgings are incorporated in Fig. 7 and compared to those of pure KCl forgings. The important features are emphasized here. First, high temperature Sr^{+2} doped forgings (Group I) exhibit no yield stress loss and no grain growth after annealing at up to 450°C. Second, normal forgings (Group II) show strength losses with annealing above 125°C. The addition of Sr^{+2} appears to decrease the rate of the strength loss with increasing temperature compared to pure KCl forgings. Third, the annealing temperature required for grain growth in normal forgings increases with the addition of Sr^{+2}.

3.3 Fracture Toughness

The average critical fracture energies, γ_c, of KCl under various conditions is reported in Table I, where γ_c was calculated from the load at which the crack was first seen to move or the maximum load on a chart recorder in tests where the crack was not being observed visually. No slow crack growth was noted during any

of these tests. In many cases, the crack jumped quickly to a new position at γ_c and then arrested until a greater load was applied.

Table I

FRACTURE ENERGIES OF KCl

Condition	γ_c, J/m^2
{100} <100> Single Crystals - air, 25°C	0.23
" " " - liq. N_2	0.25
" " " - water, 25°C	0.15
" " " - irradiated - 10^6R air, 25°C	0.35
" " " - irradiated 10^8R air, 25°C	1.0
" " " - doped, 200 ppma Sr^{+2} air, 25°C	0.6
<100> Press Forged - (6μm grain size) air, 25°C	0.6 → 3.4 (Avg. 2.0)

The value of γ_c obtained in this study for pure KCl single crystals is 0.23 J/m^2. The difference between this value and that of Westwood and Goldheim (1963) (0.11 J/m^2) appears to be due to neglect of beam rotation effects in their calculations. Single crystal values of γ_c increased by a factor of 2 to 3 when the thickness of the samples was reduced significantly. In samples less than ≈1 mm thick, calculations by Becher and Freiman (1972) indicate that the plastic zone at the crack tip extends to the free surface, allowing additional elastic energy to be absorbed in slip, thereby increasing the energy that must be added to the sample to produce crack propagation.

Preliminary results indicate that testing in liquid N_2 has almost no effect on γ_c. It also appears that the presence of water at the crack tip serves to lower the fracture energy (by $\approx$ 30 to 50%), as opposed to the increased observed by Westwood and Goldheim (1963).

Samples of pure KCl were irradiated with gamma rays from a Co-60 source to total dosages of 10^6 and 10^8R. Specimens were then prepared and tested in air in a darkened room to prevent optical bleaching. The fracture energy of KCl containing 150-200 ppma of Sr^{+2} was also measured. The results presented in Table I indicate that both irradiation and doping cause an increase in the fracture toughness of KCl single crystals.

The fracture energy of polycrystalline bodies of press forged KCl (Table I) ranged from 0.6 J/m^2 to approximately 3.4 J/m^2. The average fracture energy of material having $\approx$6μm grain size was about 2.0 J/m^2, nearly an order of magnitude greater than that of the starting crystals. The stress conditions in the polycrystalline KCl probably lay intermediate between plane stress and plane strain, depending on the yield stress of the specimen. This value could vary between 3000 to 5000 psi (20.7-34.5 MN/m^2) for these specimens, giving rise to a plastic zone size in the approximate range 0.2 mm to 0.5 mm. This variance could be one of the main factors producing the scatter in results. These thin (0.75-1.0 mm) polycrystalline samples were used because of the difficulty in obtaining thicker ones in the length and width needed in the test. No slow crack growth was observed in the press forged KCl. In fact, one sample was held for 48 hrs. at 75% of the failure load with no visible

change in crack position. It was seen, however, that a damage zone sometimes existed at the crack tip during loading. This zone appeared to consist of a large number of small flaws radiating out from the primary crack and could serve to increase the energy necessary to propagate it (Hoagland et al (1972)). Because of the easy cleavage of individual grains, such behavior is not unexpected. The tendency of the crack to veer out of the groove during propagation is probably also related to the existence of flaws along the groove edges which can propagate due to the bending moment in the arms.

4. DISCUSSION

The influence of divalent cation additions is reflected in the crystal forging behavior and subsequent annealing effects, as well as the mechanical strengthening of KCl. These are discussed in terms of (1) changes in thermal behavior which includes recovery, recrystallization, and grain growth, (2) yield strength increases and the mechanisms involved, and (3) fracture energy as affected by irradiation, as well as by alloying of crystals and by the introduction of grain boundaries.

4.1 Thermal Behavior

Understanding the forging of KCl, as well as the yield and fracture behavior of press forged KCl, requires that the effects of doping on recovery, recrystallization and grain growth also be considered. Recovery relieves stored strain energy by motion and annihilation of vacancies and dislocations. Recrystallization, which generally requires some critical stored strain level, competes

with recovery in the removal of dislocation-associated strain energy. These thermally activated processes are affected by impurities (Clareborough et al (1963)); thus, their behavior in alloyed KCl is important in considering strengthening mechanisms.

Recovery by the rearrangement of dislocations generally initiates in pure metals at ≈1/3 the absolute melting point (T_m). With minor additions of Sr^{+2} to KCl crystals, the temperature required to relieve (or recover) residual prestrain effects is raised (i.e., ≃ 0.3 T_m for pure KCl to 0.30-0.45 T_m for KCl-≦20 ppma Sr^{+2}). This indicates that strontium additions inhibit the rearrangement of dislocations during annealing, thus the removal of residual stored strain. Similar effects occur with the recrystallization of Sr^{+2} doped KCl where the addition of 1000 ppma Sr^{+2} increases the temperature for full recrystallization from 0.38 T_m for pure KCl to ≧0.47 T_m. The suppression in recovery and recrystallization, together with the retardation of grain growth with strontium additions during annealing, suggest that recrystallization is inhibited by a decrease of boundary mobility and not a decrease in nucleation by the presence of divalent strontium.

In a dynamic process where deformation, recovery and recrystallization occur simultaneously, such as press forging, it is expected that the forging strains are not completely removed. The resultant residual strains are exaggerated in doped forgings by the greater strain hardening rates, as well as inhibited recovery and recrystallization caused by the strontium additions. The observed grain growth in normal strontium doped forgings is felt to be enhanced

by this residual strain as noted in pure KCl (Becher and Rice (1972)). The high temperature doped forgings did not exhibit strain relief with annealing, indicating this is accomplished during forging. The lack of grain growth during annealing of these latter forgings gave further support for the role of residual strain in grain growth.

4.2 Yield Stress

4.2.1 SINGLE CRYSTALS

The mechanical behavior of the B single crystals is consistent with previous observations by Chin et al and Sibley et al (1972) in that the change in resolved shear stress is dependent on the concentration of Sr^{+2} to the 1/2 power at room temperature. Assuming the same behavior holds at 0°K, the tetragonal lattice elastic strain ($\Delta\epsilon$) resulting from a defect can be calculated by the model of Fleischer (1962),

$$\Delta^{\tau} = G/n\ C^{1/2} = GC^{1/2}\ \frac{\Delta\epsilon}{3} \quad ,$$

where Δ^{τ} is the change in resolved shear stress, G the shear modulus, C the mole fraction of solute (or defect), and n a factor related to $\Delta\epsilon$. These computations yield n = 15 and $\Delta\epsilon$ = 0.2 using data in Fig. 3 for B crystals, comparable to the results of Chin et al (1973). The value of n is almost an order of magnitude lower than that predicted by Fleischer (1962) for a divacancy and near that for interstitials. Therefore, mechanisms in addition to elastic lattice distortion must be entering into the strengthening of Sr^{+2} doped B crystals. The large increase in shear stress with Sr^{+2} additions (as shown by a low value of n) demonstrates the

efficiency of Sr^{+2} as a strengthening agent in the KCl crystal grown by the RAP Bridgeman technique.

4.2.2 POLYCRYSTALLINE KCl

Forgings of <100> A crystals with 200 ppma Sr^{+2} additions demonstrate that the polycrystalline yield strength is increased over that of pure <100> KCl forgings by solid solution strengthening effects (Becher and Rice (1973c)). The addition of 1000 ppma Sr^{+2} to <100> A crystals increases as-forged strengths due to solution strengthening plus an addition mechanism which appears to raise the Petch slope. The common <100> forging axis in pure KCl and doped A crystal forgings should result in similar textures, and thus texture differences cannot explain changes in the strengthening behvaior. As an example, pure KCl forged along <111> exhibits a Petch plot intermediate to and paralleling that of <100> KCl forgings and Group I forgings; at a 10μm grain size, <111> KCl forgings are ≦600 psi stronger than <100> KCl forgings. Chin and Mammel (1973) indicate that differences in texture should influence the strength of hot worked alkali halides, but these more likely change the intercept, and not the slope, of the Petch plot.

Part of the increase in the polycrystalline yield strength of <111> Sr^{+2} doped B crystal forgings may be attributed to differences in texture over that of <100> KCl forgings. The higher yield strengths of Group I <111>, as compared to <100> KCl, forgings are felt to result from solid solution strengthening and possible differences in texture. The ≈1000 psi yield strength increase in the Group I bodies at 4μm grain size can result from

a combination of the ≥500 psi increase in KCl crystal yield stress with strontium addition and the ≤600 psi increase in the yield strength of <111> versus <100> KCl forgings. These results suggest optimization of solution strengthening, and any texture effects that exist, to further improve the yield strength of polycrystalline KCl.

The question then is why do Group II Sr^{+2} doped forgings (and 1000 ppma Sr^{+2} A forgings) have a higher Petch slope, Fig. 5, than either Group I Sr^{+2} doped or pure KCl forgings? Increases in the Petch slope by chemical (or structural) changes of the grain boundaries by strontium precipitation in Group II forgings are likely ruled out as no precipitation effects were noted in B crystals below 300°C. Also, precipitation should be negligible as a result of the low impurity contamination and low strontium content in B crystals which, as suggested by Debes and Frolich (1971), would deter precipitation. Similar increases in slope of Group II by solid solution effects on grain boundaries are not expected as the Sr^{+2} contents nearly overlap with Group I (i.e., Group I has a 20 ppma lower limit and Group II an upper limit of ≈15 ppma).

The major difference appears to be the higher temperatures used to forge the Group I bodies (and the 200 ppma Sr^{+2} A forging). These higher forging temperatures have eliminated residual strain effects on the as forged Group I yield stresses. In contrast, Group II forgings do lose strength on annealing by recovery of residual strain. As compared to pure KCl forging, the recovery of residual strain is inhibited by Sr^{+2} additions. As residual

prestrains raise the apparent yield stress of KCl crystals, the same effect must occur within individual grains of forgings, thus increase the intercept value for the Petch plot. If one then uses the yield stress of prestrained B crystals for the intercept value of Group II forgings, the slope of Group II then approaches that of pure and Group I Sr^{+2} doped forgings. This suggests that the strengthening in Group II forgings is a result of an increase in lattice resistance to slip by residual strain hardening plus solid solution strengthening of the grains and not an actual increase in the slope, k.

4.3 Fracture Toughness

The nearly tenfold increase in fracture toughness produced by press forging KCl was predicted from single crystal-polycrystal effects in other materials. The observed increases in γ_c caused by irradiating and alloying appear to contradict Wiederhorn et al's (1970) results showing no effect of irradiation up to 3.38×10^7 R or doping with Ca up to 700 ppm on the fracture energy of NaCl. However, in all cases but one, Wiederhorn (1973) noted that his measurements were made on very thin samples (0.5 mm = 0.02 in). For the unirradiated pure NaCl, the yield stress is so low (150 psi, Madeau (1964)), that the plastic zone size is larger than the specimen thickness, and the specimen is in a state of plane stress. As one irradiates or dopes NaCl or KCl, its yield stress rises. At a dosage of 3×10^7 R, the yield stress of NaCl is approximately 500 psi, so that the plastic zone size is 25 times smaller, leading to a stress state intermediate between plane strain and

plane stress. In metals, such a change in the stress state would be expected to give rise to a decrease in the measured fracture energy because of plastic zone-specimen size effects (Tetelman and McEvily (1967)). In the case of most alkali halides, the room temperature plastic deformation involves fewer independent slip systems and thus not the same general ductility found in the cubic metals. Nevertheless, it is felt that the increase in measured fracture energy which would occur upon irradiation or doping of alkali halides was masked in Wiederhorn's thin samples by similar plastic zone effects. Support for this specimen size effect is indicated by the increase in fracture energy which Wiederhorn et al (1970) observed in one thicker irradiated NaCl specimen, as well as by the large γ_c's which were measured in thin KCl specimens (Becher and Freiman (1972)). The strain fields at the crack tip in the thin KCl samples are the same as that shown by Wiederhorn et al (1970) for NaCl in a state of plane strain.

Gross and Gutshall (1965) also observed an increase in the fracture energy of NaCl with an increase in F-center concentration, but they did not report specimen sizes. Bhattacharya and Zwicker (1966), however, measured a decrease in the fracture energy of KCl with Co-60 irradiation at 300°K, and an increase at 155°K. Their specimens were relatively thin, ≈1 mm, but measured fracture energies were 0.155 J/m^2 and less, much smaller than those determined in this study for the same size specimens. No complete explanation for the differences in results of the various investigators can be given at present. It appears, however, that the way in which the crack front interacts with the slip planes in the

crystals is paramount in determining fracture toughness. Normally, one would expect that a decrease in plastic deformation such as occurs upon irradiation or doping would lead to lower fracture energies, since less strain energy is used up in plastic flow. However, it appears that the limited slip systems in halides may result in focusing dislocations at the crack tip such that they aid crack growth and reduce fracture energy. In this case, impeding the motion of these dislocations, e.g., by irradiation of doping, would increase the fracture energy. Ahlquist (1973) has recently shown that fracture energy increases with yield strength for several NaCl structured materials. He has shown this is in reasonable agreement with the theory of Cottrell (1958) of nucleation of new cracks due to intersecting slip bands at the tip or ahead of the main crack. Ahlquist (1973) has also shown the authors' data is in reasonable agreement with this theory.

Although the high fracture energy of polycrystalline KCl could be due to the more tortuous crack path, part of this increase may be attributed to the impeding of dislocations by the grain boundaries, consistent with the effects found in single crystals.

5. SUMMARY AND CONCLUSIONS

The forging behavior of KCl and KCl-$SrCl_2$ crystals, especially the true stress levels required for unconstrained forgings, shows that scale-up is within present capabilities of available presses. Indeed, even constrained forgings involve only relatively low final true stress (~6500 psi) considering the strain hardening effects of

$SrCl_2$ additions. Though Sr^{+2} additions can require higher forging temperatures (300°C) to develop a polycrystalline microstructure, these do not present significant problems. Thus the technology for forging KCl crystals doped with $SrCl_2$ or other divalent cations is readily available. In fact, in view of the observed reduction in grain growth with Sr^{+2} additions, these divalent doped materials appear more attractive than KCl itself.

The enhanced yield strength and fracture energies of polycrystalline in contrast to single crystal KCl are important factors in use of KCl for optical windows. As divalent doping raises the fracture energy of KCl crystals, similar increases might be expected in the fracture energy of doped, polycrystalline KCl. The microstructural stability of press forged Sr^{+2} doped KCl with anneals to 450°C is a significant improvement over the behavior of pure KCl. These and the fact that minor additions of Sr^{+2} can further raise the yield strength of press forged KCl are seen as important additional improvements on polycrystalline materials.

Although yield strengths as high as 7500 psi were achieved in these, one must consider this is a result not only of the solid solution and possibly texture, but also of the residual strain hardening strengthening effects related to Sr^{+2} additions. This may also occur in any alloyed KCl systems. The fact that residual strain hardening can be minimized by either increased forging or annealing temperatures without necessarily incurring grain growth is also an important consideration in forging divalent doped KCl. Annealing to remove residual strains also allows one to study the

solid solution strengthening of Sr^{+2} or other additions. These suggest that incorporation of ~ 500 ppma $SrCl_2$ to KCl where the single crystal yield ($\sim\sigma_o$) can approach 2000 psi can result in polycrystalline material with a yield stress of well over the 5500 psi achieved by grain boundary and solid solution strengthening, plus the possible texture effects, in KCl-20 ppma $SrCl_2$ forgings.

In this study using a model system of Sr^{+2} doped KCl, crystals grown by the "RAP" Bridgeman technique have not only improved strength but lowered total optical absorption ($<3x10^{-4}cm^{-1}$) at 10.6μm. Forgings of similar undoped KCl have low total absorption ($\sim6x10^{-4}cm^{-1}$, Davisson (1973)) and it is expected that the strontium doped forgings are comparable. Thus these materials illustrate the improvements in optical and mechanical properties that can be expected in press forged KCl with minor divalent cation additions.

ACKNOWLEDGEMENTS

The research was supported by the Advanced Research Projects Agency of the Department of Defense and was monitored by Dr. C. M. Stickley under ARPA Order No. 2031.

REFERENCES

Ahlquist, C. N. (1973) Private communication and submitted to Acta Met.

Becher, P. F., and Freiman, S. W. (1972) Semi-Annual Report No. 1, ARPA Order 2031, Naval Research Laboratory.

Becher, P. F., and Rice, R. W. (1972) Semi-Annual Report No. 1, ARPA Order 2031, Naval Research Laboratory; (1973a) J. Appl. Phys. 44:2915; (1973b) Proc. High Power Infrared Laser Window Materials Conf., Vol. II, C. A. Pitka (ed.) AFCRL-TR-73-0372, SR No. 162: (1973c) Semi-Annual Report No. 2, ARPA Order 2031, Naval Research Laboratory.

Bhattacharya, T. K., and Zwicker, E. F. (1966) J. Appl. Phys. 37: 771.

Chin, G. Y., and Mammel, W. L. (1973) Met. Trans. 4:335.

Chin, G. Y., Van Uitert, L. G., Green, M. L., Zydzik, G. T. and Kometani, T. Y. (1973) J. Am. Ceram. Soc. 56:369.

Clarebrough, L. M., Hargreaves, M. E. and Loretto, M. H. (1963) pp. 63-120 in Recovery and Recrystallization of Metals, L. Himmel (ed.) Interscience Publishers, New York.

Cottrell, A. H. (1958) Trans AIME 212:192.

Davisson, J. W. (1973) Semi-Annual Report No. 2, ARPA Order 2031, Naval Research Laboratory.

Debes, M., and Frolich, F. (1971) Cryst. Lattice Defects 2:55.

Fleischer, R. L. (1962) Acta Met. 10:835; (1962) J. Appl. Phys. 12:3504.

Freiman, S. W., Mullville, D. R. and Mast, P. W. (1972) Report of NRL Progress (Naval Research Laboratory) 2:36.

Gross, G. E., and Gutshall, P. L. (1965) Int. J. Fract. Mech. 1: 131.

Hoagland, R. G., Hahn, G. T., Rosenfield, A. R., Simon, R. and Nicholson, G. D. (1972) Final Report, ARPA Order No. 1579, Battelle Columbus Laboratories.

Klein, P. H. (1973) Semi-Annual Report No. 2, ARPA Order 2031, Naval Research Laboratory.

Nadeau, J. S. (1964) J. Appl. Phys. 35:1248.

Shewman, P. G. (1969) Transformation in Metals, pp. 106-111, McGraw-Hill Book Co., New York.

Sibley, W. A., Rutler, C. T., Hopkins, J. R., Martin, J. J. and Miller, J. A. (1973) Annual Tech. Report, ARPA Contract No. F19628-72-C-0306, Oklahoma State Univ.

Tetelman, A. S. and McEvily, A. J. (1967) Fracture of Structural Materials, p. 132, John Wiley and Sons, New York.

Westwood, A. R. C. and Goldheim, D. L. (1963) J. Appl. Phys. 34:2085.

Wiederhorn, S. M., Moses, R. L. and Bean, B. L. (1970) J. Am. Ceram. Soc. 53:18.

Wiederhorn, S. M. (1973) Private Communication.

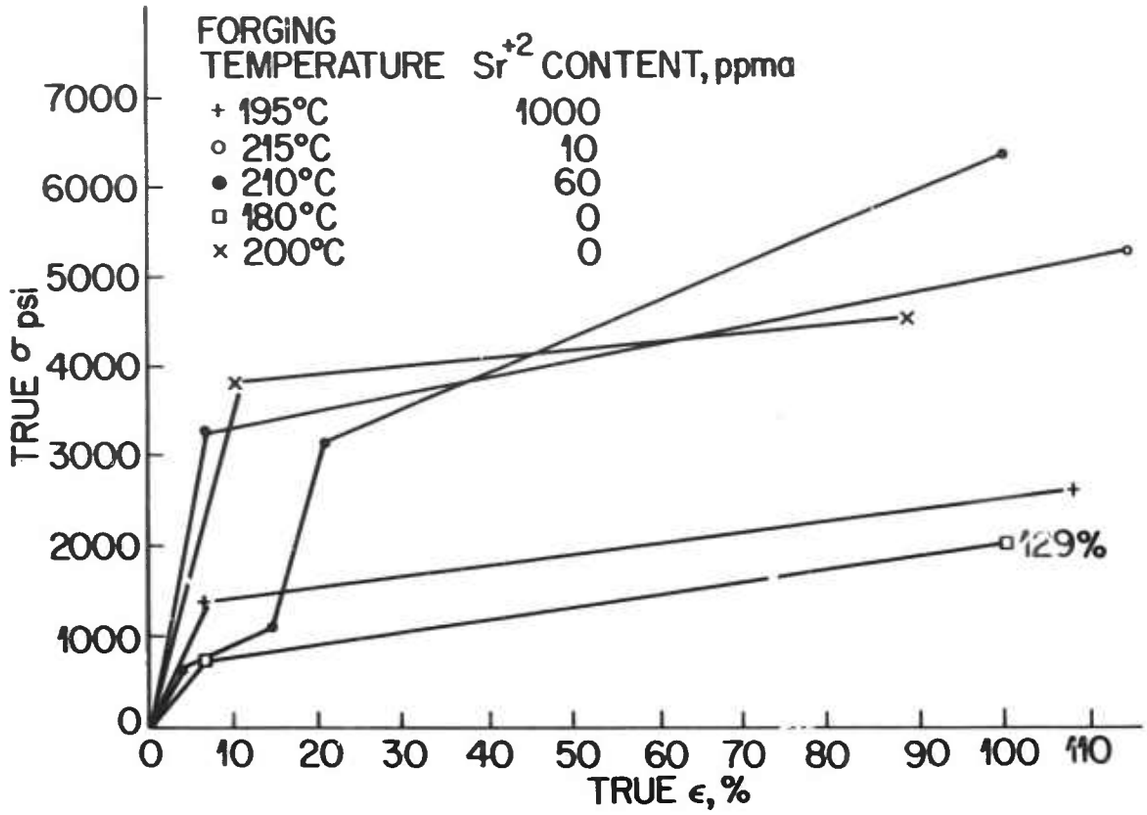

Figure 1. Stress-Strain Behavior for KCl Forgings.

These plots for two <100> unconstrained (lower) and three <111> constrained (upper plots) forgings do not include nonlinear strain hardening during forging but are representative of relative differences that occur. Constrained forging of crystals longer than the copper sleeve (60 ppma, 210°C) demonstrate yield in the copper sleeve (second yield point), not in the crystal (initial flow stress), dominates forging stresses.

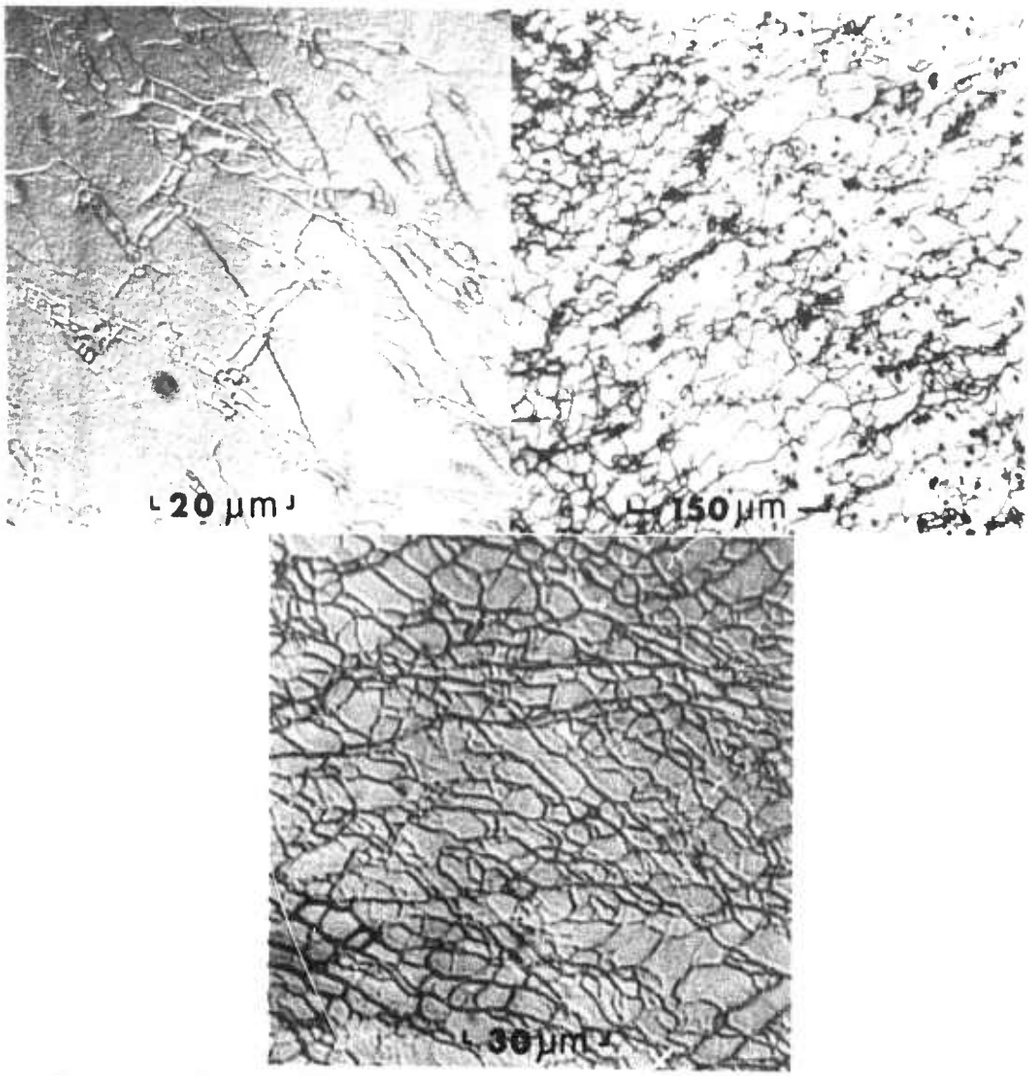

Figure 2. As Forged Microstructure of KCl-$SrCl_2$ Bodies at ≈105_2 True Strain.

The <100> A crystals with 1000 ppma $SrCl_2$ are only partially recrystallized when forged at 175°C (upper left), but fully recrystallized at 260°C (upper right). The <111> B crystals (≈15 ppma $SrCl_2$), when forged at 210°C, exhibit a homogeneous polycrystalline microstructure (lower).

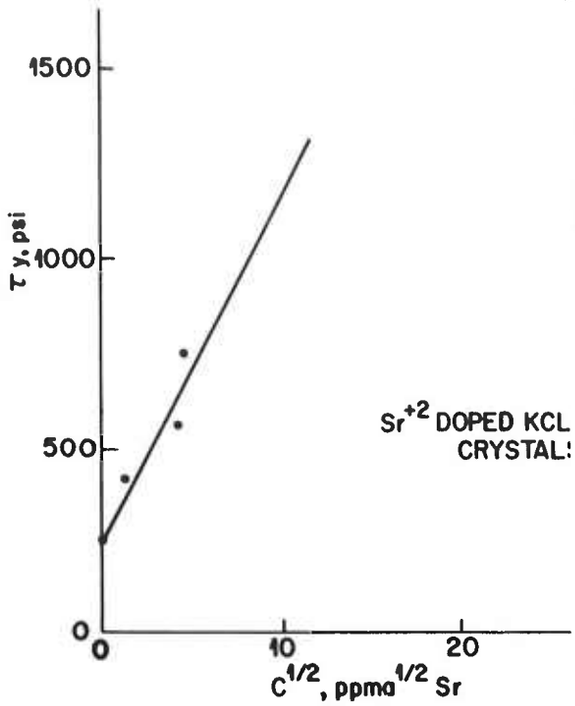

Figure 3. Effect of Sr^{+2} on the Resolved Shear Stress of KCl Crystals.

The stress is resolved for {110}<110> slip, and the strontium contents are as measured in these RAP-Bridgman grown crystals.

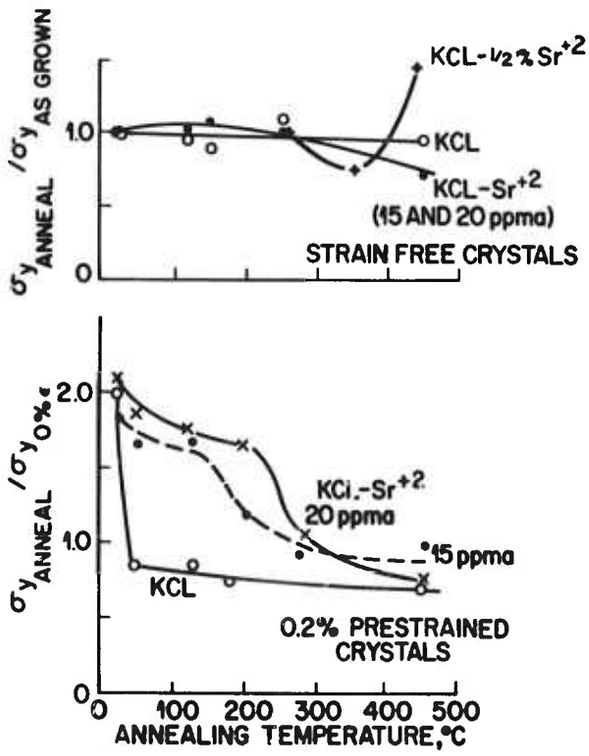

Figure 4. Annealing Temperature Effects on Single Crystal Yield Stress.

As-grown crystals were annealed to observe precipitation softening effects (upper graph) while recovery (strain relief) was indicated by the loss of the yield stress increase caused by prestraining (lower graph).

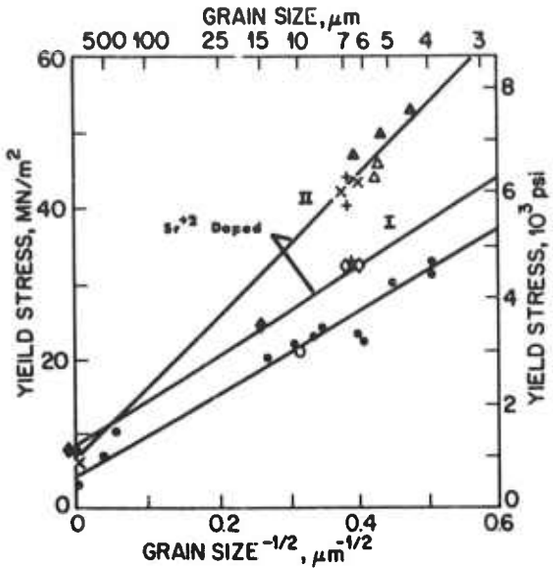

Figure 5. Yield Strength-Grain Size for Sr^{+2} Doped and Pure KCl.

The polycrystalline bodies were produced by press forging <111> RAP Bridgman grown Sr^{+2} doped as well as commercially available <100> KCl crystals.

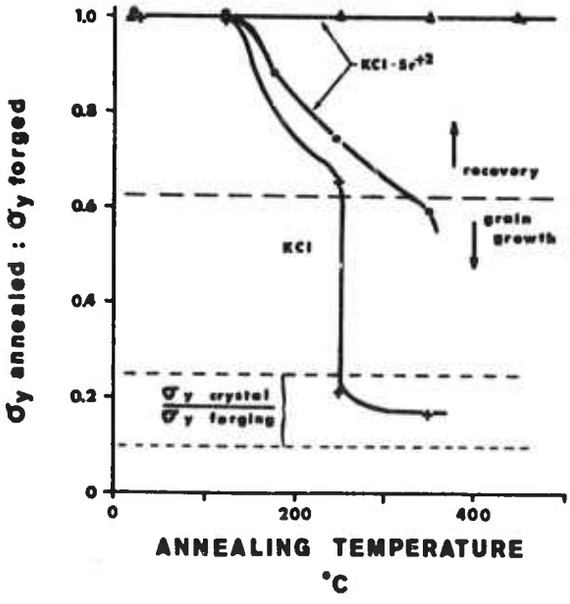

Figure 6. Ratio of As Annealed to As Forged Yield Strength of Press Forged KCl.

The Sr^{+2} doped forgings from B crystals contain >10 to <25 ppma Sr^{+2}. Prior to any observed grain growth, the grain size of all forgings was 5 to 8μm, which rapidly increased to >100μm when grain growth occurred.

GROWTH, FINISHING, AND OPTICAL ABSORPTION OF PURE POTASSIUM CHLORIDE SINGLE CRYSTALS*

J. W. DAVISSON, M. HASS,
P. H. KLEIN and M. KRULFELD
U. S. Naval Research Laboratory
Washington, D. C. 20375

Abstract

Single crystals of potassium chloride, 2.5 cm in diameter and 4-11 cm long, have routinely been prepared with calorimetrically-determined absorption coefficients smaller than 0.0002 cm^{-1} at 10.6 μm. These crystals have been grown in a carbon-tetrachloride-saturated atmosphere by the Bridgman method, using an adaptation of the Reactive Atmosphere Process introduced by R. Pastor at Hughes Research Laboratory. Use of finishing techniques which minimize abrasion has made it possible to prepare ingots with measured absorption coefficients on occasion as low as 0.00012-0.00015 cm^{-1}. (No surface corrections--which would tend to decrease the value obtained--have been applied to the absorption coefficients reported here.) Presumably, the special finishing techniques avert introduction of those absorbing centers which might result from cleaving of crystals. Measurements as a function of length indicate that surface absorption is small, although reproducible values are difficult to obtain at such low total-absorption levels. On the basis of these data, coupled with absorption measurements as a function of temperature, it is believed that the bulk 10.6 μm absorption in these crystals is close to the estimated intrinsic level ($\beta = 0.00008$ cm^{-1}).

*Work partially supported by Advanced Research Projects Agency under ARPA Order 2031.

1. INTRODUCTION

Theoretical and experimental investigations of optical distortion in cw high power CO_2 laser windows indicate that potassium chloride is the best candidate material available at this time. Here the parameter most subject to uncertainty is the value of the absorption coefficient. Since the reported absorption coefficients from materials from different sources is quite variable and above the estimated intrinsic limit, it appears that materials development is capable of substantial improvements. In this investigation, the growth, finishing, and infrared absorption of pure potassium chloride single crystals having absorption coefficients less than 0.0002 cm^{-1} is described. Furthermore, the difference between the measured value and the estimated intrinsic limit of 0.0008 cm^{-1} might be ascribed to surface absorption, i.e., the bulk absorption in these crystals might be very close to the intrinsic level.

2. CRYSTAL GROWTH

The apparatus used at the Naval Research Laboratory for growth of single crystals of KCl is shown schematically in Figure 1 and photographically in Figure 2. The equipment is an adaptation of that used at Hughes Laboratory by R. Pastor [Pastor and Braunstein (1973)] and employs the "Reactive Atmosphere Process"(RAP) described by him. This procedure is a variant on halogen-purification of alkali halides, whereby the nascent halogen is derived from thermal cracking of carbon tetrachloride [Rosenberger (1972)]. Displacement of OH impurities from the salt by the halogen (as well as some transport of metallic impurities in the flowing gas) is believed to be the means whereby the KCl is purified. As shown in Table I, 10.6-micrometer absorption coefficients in the 0.00015-0.00030 cm^{-1} range are routinely obtained.

In use, the Vycor crucible is charged with finely-crystalline KCl (reagent-grade Baker and Adamson, J.T. Baker, or "Suprapur"-grade E. Merck) which has been dried at 250°C. After purging with Ti-gettered, CCl_4-saturated argon, the furnace is heated to about 300°C while surrounding the crucible, and then elevated after about an hour. When the charge has cooled, the furnace is again lowered, and another thermal cycle carried out. The process is repeated at about 600°C. It is believed that these thermal cycles foster mixing of the

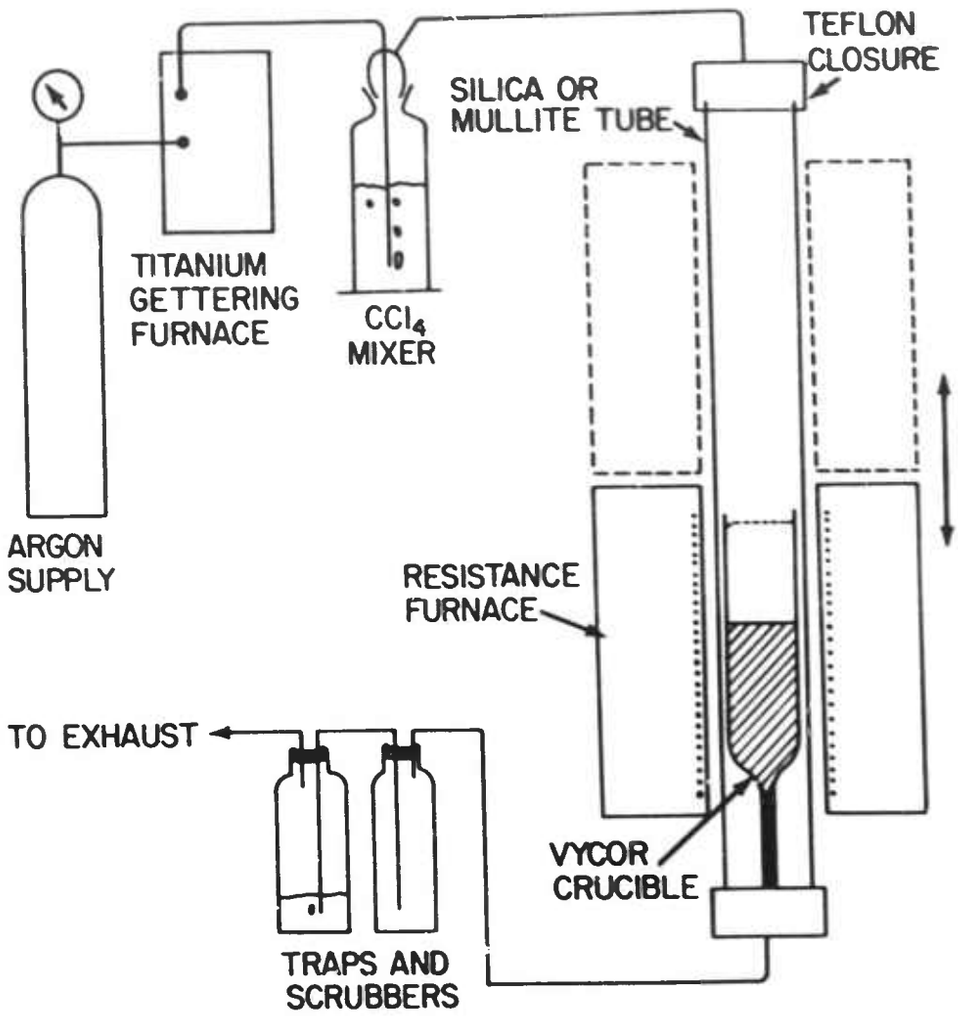

Fig. 1. Schematic diagram of system used for Bridgman growth of KCl in a reactive atmosphere.

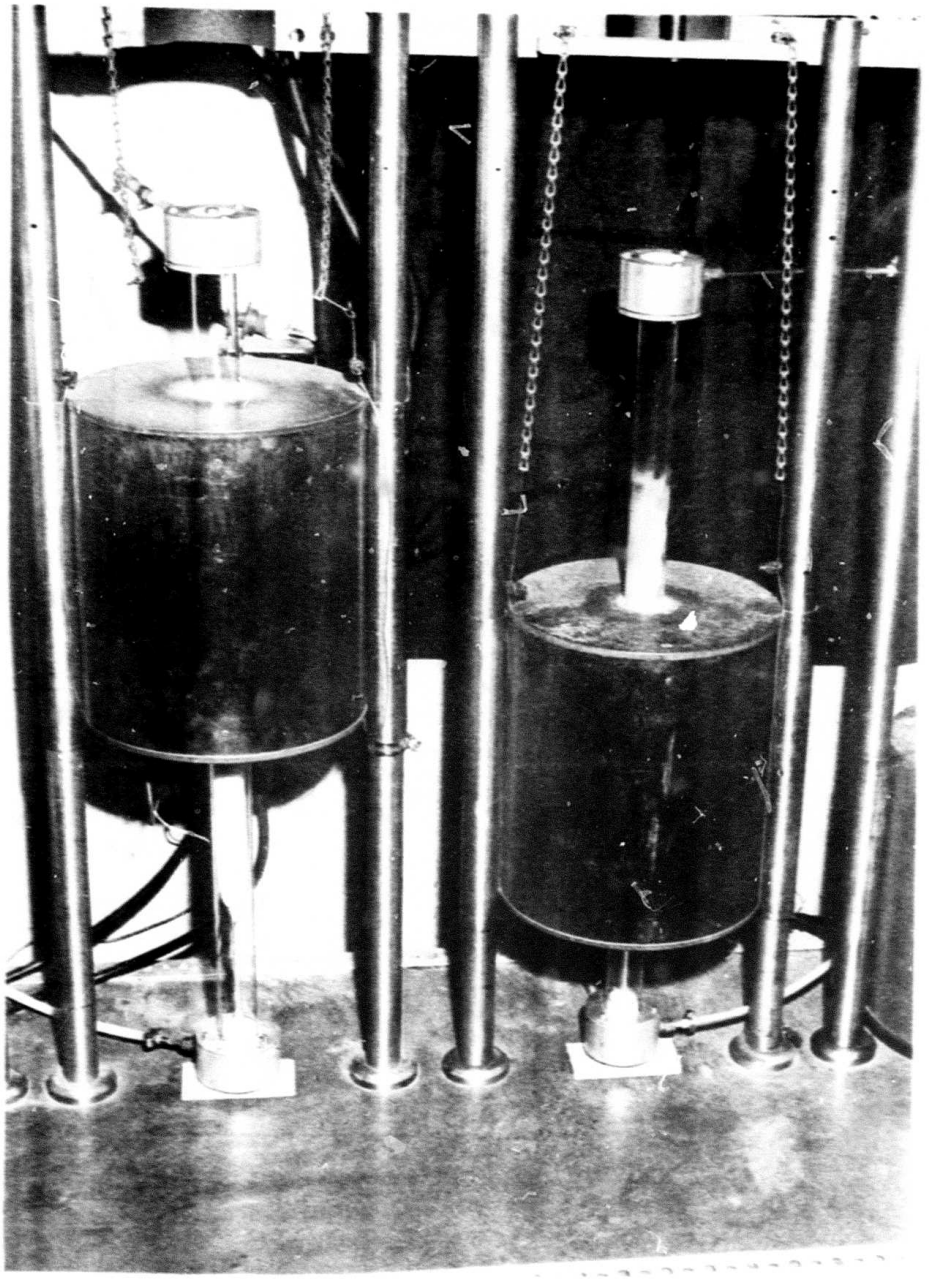

Fig. 2. Two Bridgman furnaces, suspended by chains from their elevating mechanisms. That at the left has been raised to show the position of the pointed crucible within the silica envelope prior to melting of the charge. The furnace at the right is in position for the start of a run.

halogen with the KCl while the solid has a large reactive surface area.

After two or more heating cycles at 600°C, the furnace is positioned around the charge, which then is melted. After three hours in this position, the furnace is raised at a rate of about 0.15 cm/h, eventually reaching the position shown by the dotted outline in Figure 1. When cool, the crucible is removed and customarily emptied of the facetted crystal it usually contains by careful inversion. A crust of carbon and other impurities is removed from the top and the point is removed from the bottom by use of a water-string saw, and polishing begun.

3. SURFACE FINISHING

The question of surface finishing in alkali halides is recognized to be one of the crucial aspects in the utilization of alkali halides as laser windows. While the NRL program has not been focused towards the surface finishing area, the finishing aspects are intimately associated with measurements of bulk absorption. In the course of developing good surface finishes for absorption measurements, a method of chemical polishing has been developed at NRL [Davisson (1972)]. This method provides scratch free surfaces of excellent quality. In the past year low loss crystals have become available and the technique refined further to show that these finishing techniques introduce little or no absorption at the surface as well.

It has been pointed out by various investigators that finishing procedures can introduce surface absorption [Deutsch and Rudko (1972)] and bulk absorption from operations such as cleavage [Pastor, et al. (1972)]. Procedures have been developed at NRL which avoid cleavage or other operations which might introduce absorbing centers. There are various ways of achieving this and the latest method of achieving this at NRL is described below:

(1) Sawing: A water-soaked string saw (South Bay Technology) has been found to be suitable.

(2) Grinding: Grinding to render the faces plane parallel was performed by hand using a water charged Politex "Supreme" polishing poromeric lap (Geoscience Instruments Corp) attached to a glass plate. The lap was treated with a wetting agent aerosol.

(3) Chemical Polishing: This involves immersion of the crystal in concentrated hydrochloric acid for 30 minutes. It was then washed with a jet of

ethyl alcohol and dried with a jet of dry air.

It should be emphasized that this method of finishing is relatively simple. The results to be discussed shortly suggest that there is still some residual surface absorption. The reasons for this are not completely clear. Possibly there is still some residue from the chemical polishing procedure which has not been completely removed in the washing and drying procedure.

4. RESULTS

The results of the growth and finishing techniques are best illustrated in Table I in which the absorption coefficients of various KCl ingots are shown. These were determinally calorimetrically using CO_2 laser sources[Hass, et al. (1972)].

The main point to note is that low loss crystals can be readily and reproducibly prepared by this technique in the diameters and lengths indicated. At NRL some difficulty was obtained in producing longer crystals, but this might very well be due to limitations in the length of the oven.

In addition to the pure ingots some strontium-doped ingots have also been produced. The absorption coefficients of these are also shown in Table I. The important thing to note is that the absorption coefficients of these lightly doped samples are also quite low. It is not clear what the difference between pure and doped materials can be attributed.

The above absorption coefficients were obtained by dividing the fractional power absorbed as obtained from a calorimetry measurement and dividing by the length. If carried out correctly, such an approach gives a maximum absorption coefficient as surface absorption, if any, is included. As noted by Deutsch [Deutsch and Rudko (1972)] measurements as a function of length can in principle serve to separate out the surface and bulk absorption, provided no additional bulk absorption is introduced in processing the crystals.

A few cases have been studied in this manner and an example is shown in Figure 3. If the measurements of the fractional power absorbed as a function of length are analysed, then a bulk absorption of about 0.00008 cm^{-1} and a fractional surface absorption of about 0.00012/surface can be extracted. If this procedure is valid, then it might be claimed that bulk absorption is down to the level predicted by the exponential law [Deutsch (1971).]

Table 1. Absorption coefficient at 10.6 μm of KCl single crystals grown in argon-CCl_4 ambient - arranged chronologically

Crystal Number	Starting Material	Optical Length cm	10.6-μm Absorption Coefficient, cm^{-1}	Remarks
B2	B&A	7.8 1.5	0.00015 0.00032	Crystal measured after cutting away parts
B3	B&A	7.4	0.00018	
B4	B&A	8.0	0.00024	60 ppmA $SrCl_2$ in melt
B5	B&A	5.2	0.00025	100 ppmA $SrCl_2$ in melt
B6	B&A	5.1	0.00024	10 ppmA $SrCl_2$ in melt
B7	Merck	---	---	Crystal not measured
B8	NRL purif.	---	---	Crystal not measured
B9	E. Merck	4.9	0.00060	
B10	B&A	4.6	0.00024	
B11	B&A	8.9	0.00018	
B12	B&A	4.9	0.00020	
B13	B&A	10.8	0.00015	
B14	JT Baker	2.5	0.00031	
B15	B&A	4.5	0.00014	
B16	E. Merck	5.0	0.00016	
B17	B&A	10.0	0.00012	
B201	Baker	4.9	0.00038	
B301	B&A	4.5	0.00020	
B202	B&A	5.0	0.00016	100 ppmA $SrCl_2$ in melt
B302	B&A	5.0	0.00019	
B203	B&A	5.0	0.0005	
B303	B&A	8.0	0.0006	80 ppmA $SrCl_2$ in melt
B204	B&A	5.0	0.00016	
B304	B&A	4.0	0.00027	200 ppmA $SrCl_2$ in melt
B205	B&A	5.0	0.00013	
B305	B&A	4.0	0.0005	25 ppmA $SrCl_2$ in melt
B206	B&A	5.0	0.00020	

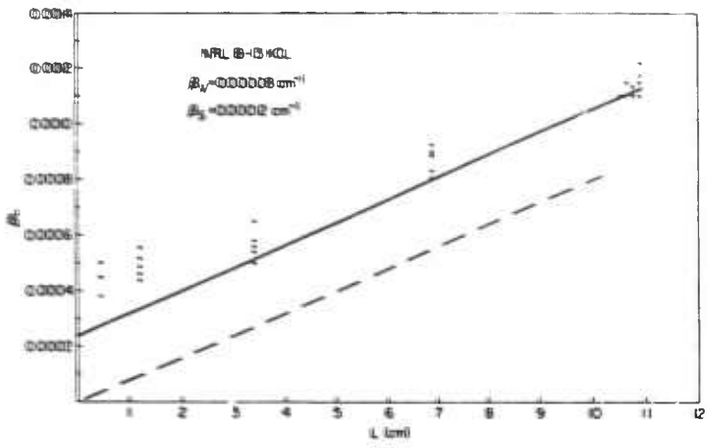

Fig. 3. Absorption coefficient of a lowloss single crystal KCl grown at NRL as a function of length. A bulk absorption coefficient (β_v) of about 0.00008 cm^{-1} can be extracted.

It should be pointed out that the results obtained reported in Figure 3 have represented several attempts, not all of which have yielded such a low absorption coefficient. Here some difficulty was experienced in obtaining low values of the surface absorption. On some days, this was due to high humidity conditions. It is believed some improvements are still possible to achieve more reproducible and lower absorbing surfaces.

In considering measurements of this nature, possible sources of error should be considered. First, it should be pointed out that some error might have entered into the calorimetric measurement. Here it might be pointed out that calorimetry is really only valid under certain conditions. For a long thin cylinder, it has been shown both experimentally and theoretically that measurement of the surface temperature gives a valid result for bulk absorption [White and Midwinter (1973)]. Where the thermal conductivity is high, geometric considerations can be relaxed somewhat. At least for the alkali halides, it has been shown that use of cube shaped samples of a few cm length will not cause any drastic errors [Hass, et al. (1972)].

In order to demonstrate intrinsic absorption, both the frequency and temperature dependence can be employed. Measurements of the frequency dependence near 10.6 μm are being carried out at NRL by L. Boyer who finds evidence of a band at 9.8 μm even in the better samples. It is not yet established whether this is associated with the surface or the bulk.

The temperature dependence of the absorption has been reported by Harrington and Hass (1973). Here a sample having an absorption coefficient of 0.0002 cm^{-1} was employed (no surface correction). The temperature dependence did increase monotonically from room temperature. If it is assumed that the temperature dependence of the intrinsic absorption is different from the extrinsic absorption, the results suggest the absorption was largely intrinsic.

In conclusion, it has been shown that pure KCl ingots can be reliably grown, polished, and measured with absorption coefficients less than 0.0002 cm^{-1}. In a specimen having absorption coefficients as low as 0.0001? cm^{-1}, measurements as a function of length indicate some surface contributions so that the bulk absorption may be less than 0.0001 cm^{-1} which is close to the intrinsic limit. Evidence based upon temperature dependence of the absorption on these crystals support this contention.

ACKNOWLEDGMENTS

The authors would like to thank J. A. Harrington who contributed heavily to many phases of this work and R. Pastor for discussions about Reactive Atmosphere Processing. They would also like to express their appreciation to Oscar Imber who was involved in the growth of the first ingot and Fred von Batchelder who grew a number of subsequent ingots.

REFERENCES

Davisson, J. W. (1972). "Chemical Polishing of NaCl and KCl Laser Windows" from 1972 Conference on High Power Infrared Laser Window Materials, AFCRL-TR-73-0372 (II) (19 June 1973), edited by C. A. Pitha, p. 525. See also "High Energy Laser Windows", Semiannual Report No. 1 and 2, (1973), ARPA Order No. 2031, Naval Research Laboratory.

Deutsch, T. F. (1971). "Optical Materials and Structures for High Power Lasers (II). Experimental". from 1971 Conference on High Power Infrared Laser Window Materials. AFCRL-71-0792 (13 December 1971), edited by C. S. Sahagian and C. A. Pitha, p. 55; See also J. Phys. Chem. Solids (in press).

Deutsch, T. F. and Rudko, R. I. (1972). "Bulk and Surface Absorption in Infrared Laser Windows" from 1972 Conference on High Power Infrared Laser Window Materials, AFCRL-TR-0372 (I), (19 June 1973), edited by C. A. Pitha, p. 201.

Harrington, J. A. and Hass, M. (1973). "Temperature Dependence of Multiphonon Absorption", Physical Review Letters 31, 710; see also 1973 Conference on High Power Infrared Laser Window Materials.

Hass, M., Patten, F. W., and Rosenstock, H. B. (1972). "Lattice Absorption in Transparent Crystals", from 1972 Conference on High Power Laser Window Materials, AFCRL-TR-0372 (I) (19 June 1973), edited by C. A. Pitha, p. 176.

Pastor, R. C. and Braunstein, M. (1973). "Advanced Mode Control and High Power Optics Technology" AFWL-TR-152 Vol. II, Hughes Research Laboratory, Malibu, California.

Pastor, R. C., Pastor, A. C., and Kiefer, J. E. (1972). "Optical Absorption of Potassium Chloride and Ten Microns" from 1972 Conference on High Power Infrared Laser Window Materials. AFCRL-TR-0372 (II) (19 June 1973), edited by C. A. Pitha, p. 535.

Rosenberger, F. (1972). "Purification of Alkali Halides", from Ultrapurity: Methods and Techniques, edited by M. Zief and R. M. Speights, Dekker.

White, K. I. and Midwinter, J. E. (1973). "An Improved Technique for the Measurement of Low Optical Absorption Losses in Bulk Glass", Optoelectronics, 321.

TUNABLE ABSORPTION IN KCl NEAR 10.6μm.

Since completion of the above manuscript, some preliminary absorption measurements as a function of frequency have been carried out at NRL by Larry L. Boyer using a tunable CO_2 laser. A discussion of these results is given here.

The wavelength dependence of the absorption coefficient (uncorrected for surface effects) of a good KCl crystal having an absorption coefficient of about 0.0002 cm^{-1} near 10.6 μm is shown in Fig. 4. It can be seen that there is an absorption band at about 9.8μ which has been observed elsewhere in surface absorption and emissivity studies. The absorption level of this band appears to vary more strongly from point to point and from sample to sample than does the absorption at 10.6μm. At present, this suggests that this band might be associated in part or completely with some surface effect.

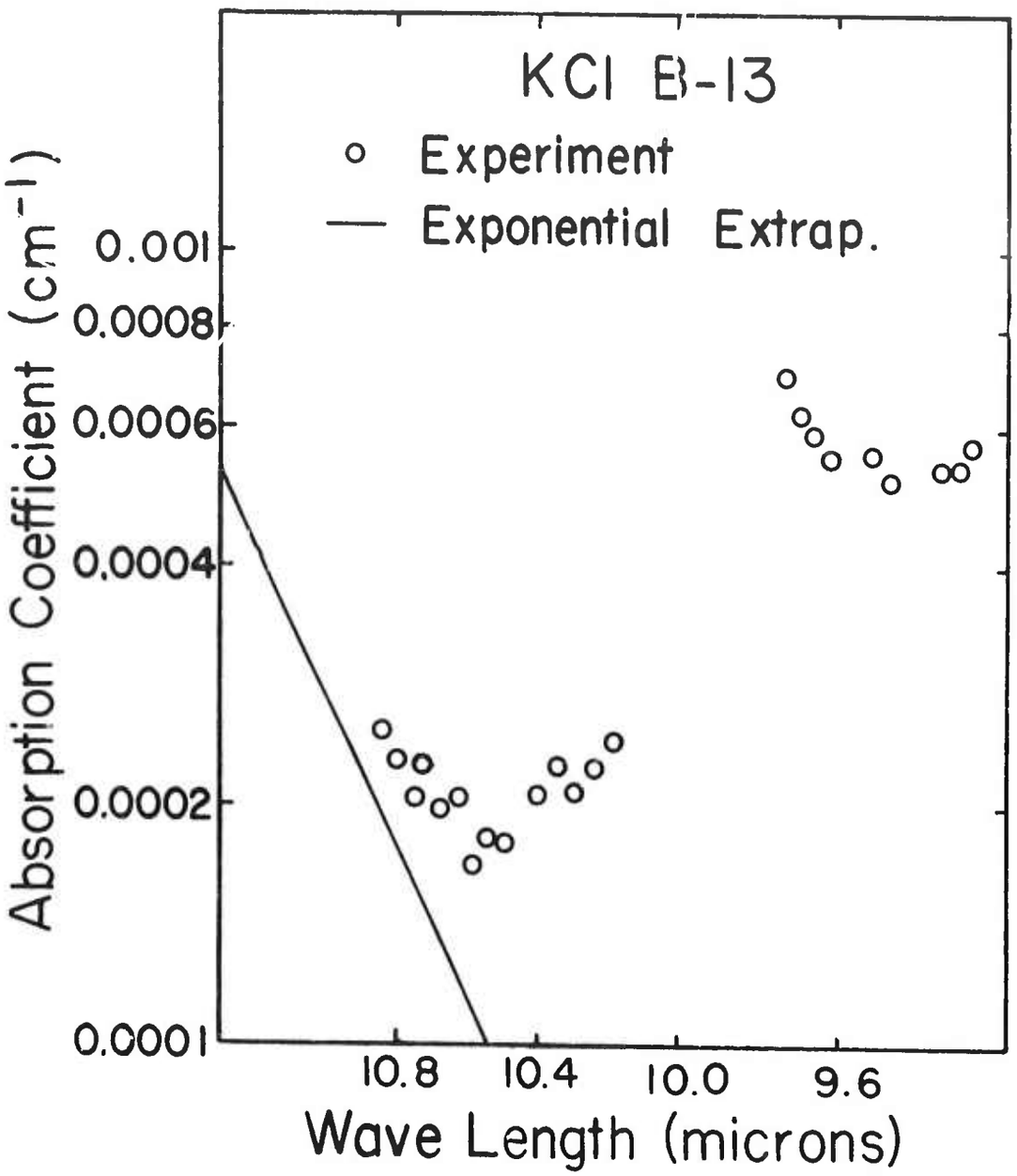

Fig. 4. Absorption coefficient of NRL sample B-13 of KCl as a function of wave length. Circles are the experimental data obtained using the laser calorimetric technique with a tunable CO_2 laser. The solid line is the exponential absorption extrapolated to the 10.6 micron region.

TEMPERATURE DEPENDENCE OF MULTIPHONON ABSORPTION

JAMES A. HARRINGTON
and MARVIN HASS
U.S. Naval Research Laboratory
Washington, D.C. 20375

Abstract

Studies of the temperature dependence of absorption of laser window materials are of importance in distinguishing between intrinsic and extrinsic absorption as well as being essential in evaluating various theoretical calculations of the absorption. The absorption coefficients of KCl, NaCl, and NaF have been measured at 10.6 μm from room temperature to just below the melting point. For NaF, NaCl, and a good sample of KCl (room temperature coefficient $\sim 0.0002\ cm^{-1}$), the absorption increases with temperature and at higher temperatures can be represented by the expression T^x, where x = 1.6 for NaF, 2.3 for NaCl, and 2.3 for KCl. For samples of KCl having higher room temperature coefficients, the absorption has been observed to be approximately independent of temperature or even decrease with temperature. These results are interpreted as indicative of near intrinsic behavior for NaF, NaCl, and the good sample of KCl. For the higher loss KCl samples, impurity or defect absorption appears dominant. The temperature dependence of the intrinsic absorption can not be explained by use of simple Bose-Einstein populations factors which has served satisfactorily for semiconductors. The data can be explained by more complete theories in which the large anharmonic effects of alkali halides are taken into account.

*Supported in part by the Advanced Research Projects Agency under ARPA Order No. 2031.

1. INTRODUCTION

Multiphonon absorption is generally believed to account for the residual absorption in infrared for many laser window materials, especially those for the 10.6 μm region. Studies of the frequency and temperature dependence of the absorption can provide a means for distinguishing between intrinsic and extrinsic effects. Since the absorption coefficients of good laser window materials are very low, it is difficult to study the frequency dependence over a wide wavelength range at this time. However, using calorimetric absorption techniques with laser sources, it is possible to study the temperature dependence of the absorption at fixed frequency. Previous investigations of multiphonon absorption in the III-V compounds have shown that the experimentally observed temperature dependences at fixed frequency could be explained using only simple Bose-Einstein population factors. Initially, it was thought that this approach could be extended to the alkali halides. The experiments reported here have been stimulated by this expectation.

In order to investigate the validity of the approach, studies of the temperature dependence of the absorption of NaF, NaCl, and KCl were undertaken. Briefly, the results have shown that the temperature dependence of the intrinsic absorption of these materials can not be represented by use of simple Bose-Einstein population factors. As a result of this work, a number of theoretical calculations of the absorption have been extended in order to obtain agreement with the experimental results. It appears that the large amount of anharmonicity in the alkali halides results in temperature dependent lattice frequencies and possibly other factors which preclude use of simple Bose-Einstein factors.

The principal results of this work have been reported recently in the literature [Harrington and Hass (1973)] and will not be repeated here. In this report, the following aspects will be emphasized: (1) a description of the experimental arrangement; (2) experimental results; and (3) discussion in regards to the laser window program.

2. EXPERIMENTAL ARRANGEMENT

The determination of the temperature dependence of the absorption is important because it provides a check on one of the basic assumptions of the theory. If simple Bose-Einstein population factors are employed to predict the temperature dependence of the absorption, then large effects can be expected in the high temperature region. However, the experimental determination of such absorption coefficients in the high temperature region has not been reported previously. At the time these experiments were attempted, it was not clear whether these measurements would be possible, as small temperature differences in the range of tenths of a degree are measured. However, it was found that laser calorimetric techniques can be modified for high temperatures in the following way.

The special high temperature calorimeter, constructed for measurements of β from room temperature to within $50^{\circ}K$ of the sample's melting point, consisted of a horizontal core furnace with an API controller. In order to have the good thermal stability required for calorimetry, the sample was placed in a large thermal mass (a 2" o.d. x 1" i.d. x 4" stainless steel cylinder with four asbestos support screws to hold the sample), which was in turn placed inside a stainless steel box to minimize convection currents. This entire assembly was then loaded into the furnace. Using this arrangement, it was possible to achieve an ambient temperature stable to within half a degree of $1000^{\circ}K$ or to within a few tenths of a degree at $500^{\circ}K$.

To measure the small change in temperature produced by either laser or resistor (see below) heating at elevated temperatures, it was necessary to modify our usual method of thermolcouple attachment. In this case, 5 mil chromel-alumel thermocouples were imbedded in a small hole (No. 70) drilled in the crystal. Sauereisen cement was used to maintain good thermal contact between the crystal and thermocouple at high temperatures. The reference junction was similarly attached to the thermal mass.

The entire experimental setup for high temperature calorimetry is shown schematically in Fig. 1. In addition to the calorimeter described above, the setup includes our standard signal detection equipment: a Keithley Model 149 milli-microvoltmeter and HP strip chart recorder for monitoring the differential temperature changes and a CRL laser power meter. The absorption

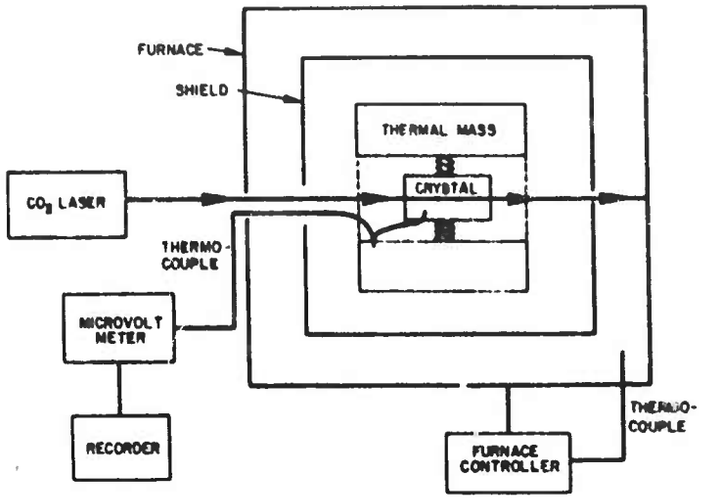

Fig. 1. High temperature calorimetry system.

coefficient was evaluated from the heating and cooling curve using the "three-slope" method [Hass and Patten (1972)].

Measurements of β as a function of temperature in NaF were not made calorimetrically because of the high value (0.6 cm^{-1}) of β at 10.6 μm (300°K). Instead, β as a function of temperature was measured optically simply by measuring the incident and transmitted laser power with the power meter.

In KCl, NaCl, and NaF, care was taken to insure that surface degradation at elevated temperatures was minimized. Since all measurements were made in air, surface effects at the highest temperatures could be a problem. Initially, the crystals were chemically polished. In the process of data taking, the temperature would occasionally be recycled to a lower value and β remeasured to check for surface absorption. In many cases the value of β obtained on recycling was less than the original value, but this can be explained in terms of an annealing out of absorbing imperfection centers. In any case, the highest temperature was very near the melting point and at that point, data taking was terminated.

As a means of checking on the reliability of our high temperature calorimetric results, we replaced laser heating with electrical heating in KCl and measured the specific heat, C_p, as a function of temperature. Such a measurement of C_p and comparison against accepted values would provide a check of our apparatus. A resistor, fabricated using a porcelain core and 3 mil chromel wire, was imbedded and cemented with Sauereisen into a KCl crystal. The results of C_p as a function of temperature are given in Table 1. It can be seen that, while the agreement is not as good as one would desire, the measured values are not so different from the accepted values so as to lead us to seriously doubt the validity of our high temperature calorimetric measurements.

Table 1

Specific Heat of KCl as a Function of Temperature

T (°K)	C_p Observed (J/gr · °K)	C_p Accepted (J/gr · °K)
298	0.583	0.6835
470	0.690	0.736
655	0.88	0.760

3. EXPERIMENTAL RESULTS

The temperature dependence of the absorption in NaF, and NaCl, and KCl are shown in Figs. 2-5. For NaF and NaCl, the absorption increases monotonically with temperature and is believed to be largely intrinsic in origin. The solid curves represent that predicted simple Bose-Einstein population factors.

For KCl, the results are more complicated. For this compound, the measurements varied from sample to sample as shown in Fig. 4. In some cases, the absorption was essentially independent of temperature, while in one sample the absorption appear to even decrease with temperature, possibly due to annealing effects. In the best sample available at the time (from Hughes Research Laboratory), the results above 500^{o}K did indicate a large temperature dependence expected for intrinsic absorption.

Encouraged by this result, further experiments were undertaken. The increased availability of low-loss boules grown using the Hughes approach at NRL [Davisson et al. (1973)] coupled with improvements in chemical polishing have led to the preparation of a crystal having a lower room temperature absorption coefficient of about 0.0002 cm^{-1}, where no surface absorption has been subtracted out. Such a sample might be expected to display a large temperature dependence of the absorption expected from theoretical considerations. The experimental results are shown in Fig. 5. It can be seen that the temperature dependence of this sample resembles that of NaF and NaCl in being essentially monotonic even near room temperature. The absorption can be represented as being proportional to $T^{2.3}$, which is slightly higher than the value of $T^{1.8}$ reported for the Hughes sample at high temperatures. The differences between the Hughes and NRL sample might be very well associated with the surface polishing procedure.

4. DISCUSSION

Studies of the temperature dependence of the multiphonon absorption are of interest in the following areas of the laser window program: (1) determination of the intrinsic absorption in window materials; (2) discrimination between intrinsic and extrinsic absorption.

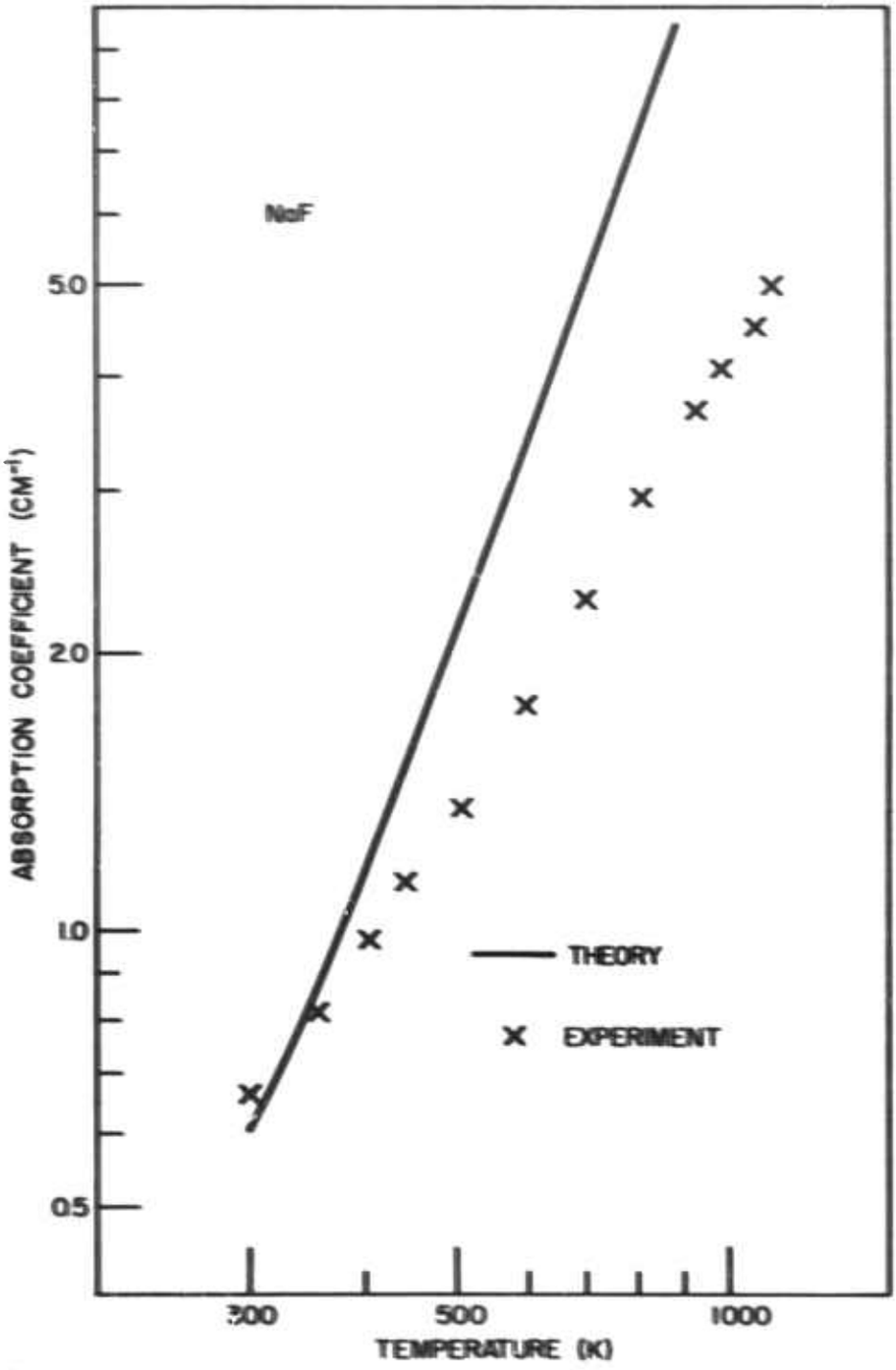

Fig. 2. Temperature dependence of absorption coefficient for NaF. The solid line is the temperature dependence calculated using Bose-Einstein population factors.

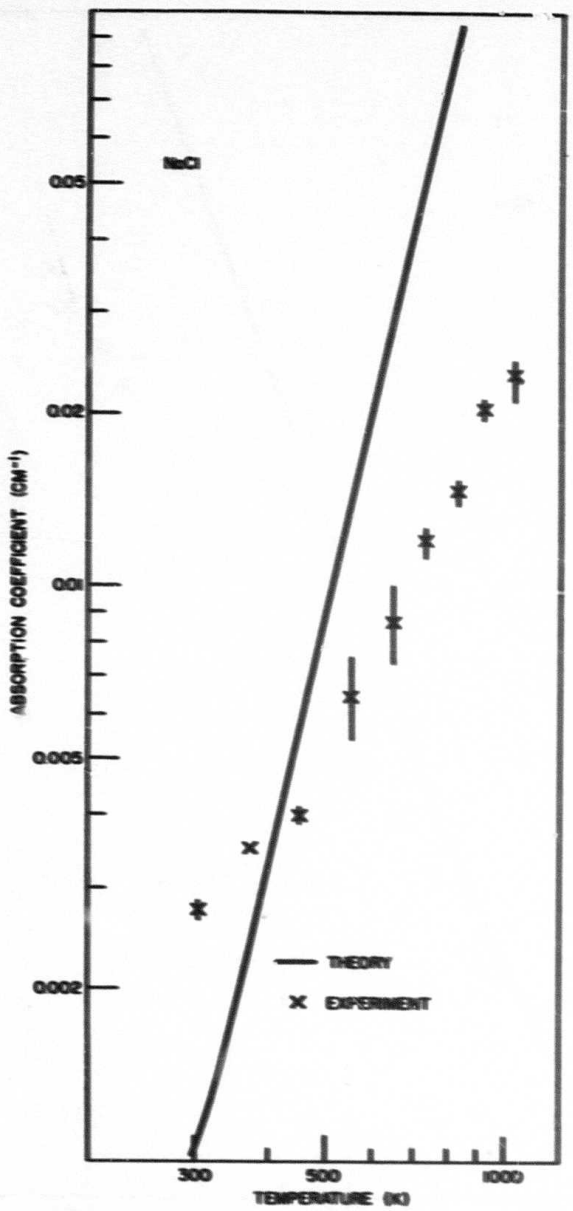

Fig. 3. Temperature dependence of absorption coefficient for NaCl. The solid line is the temperature dependence calculated using Bose-Einstein population factors.

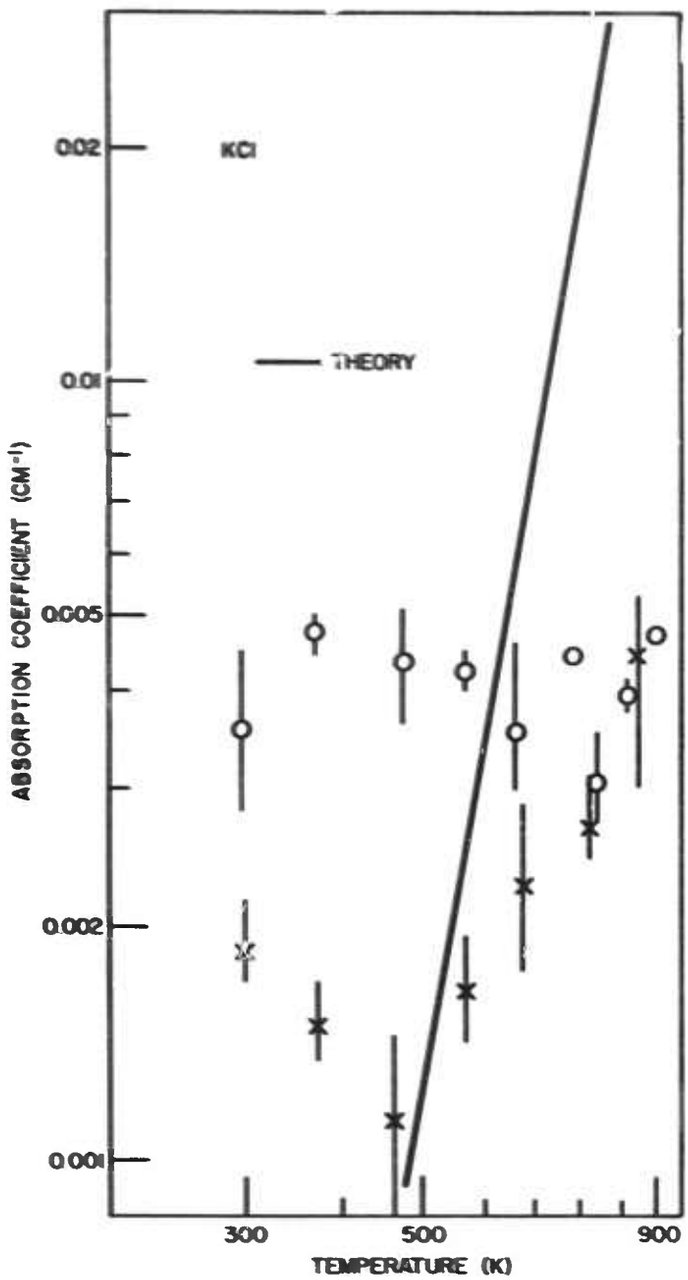

Fig. 4. Temperature dependence of absorption coefficient for KCl. The open circles are data from Harshaw KCl, the crosses data from a KCl sample obtained from Hughes Research Labs., Malibu. The temperature dependence calculated using Bose-Einstein population factors.

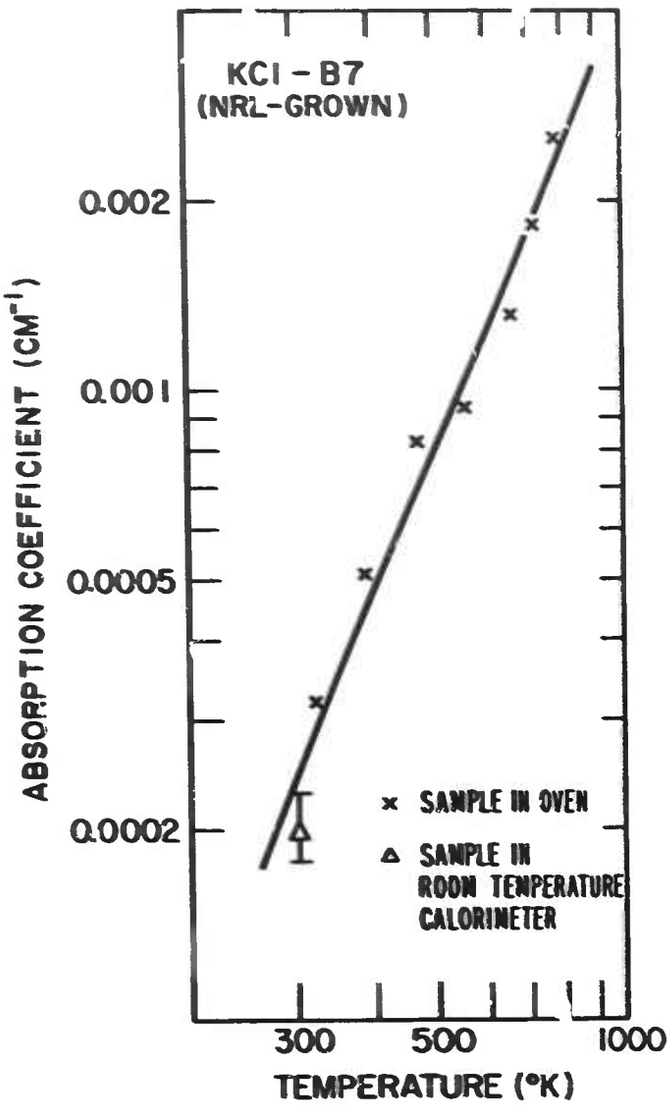

Fig. 5. Temperature dependence of absorption coefficient for KCl (grown at NRL). The solid line is drawn through the data and is not deduced from theory.

4.1 Determination of Intrinsic Absorption

The determination of the magnitude of the intrinsic absorption at the laser frequencies in window materials is of considerable interest in establishing a goal for the crystal grower. In selecting an estimate for the intrinsic absorption, reliance has been placed upon the experimental observation of an exponential dependence of the absorption as a function of frequency on the high frequency side of the absorption band in many materials. By extrapolation, an estimate of the absorption coefficients at various wavelengths can be made. [Deutsch (1971). Although there is no evidence at present to cast doubt on this procedure, it is not based upon any rigorous theoretical justification. Current theoretical calculations of the absorption have shown that a frequency behavior close to exponential can be obtained, but these are still based upon a number of approximations. However, the ability of a theoretical calculation to predict correctly both the frequency and temperature dependence places somewhat more confidence in the results.

A discussion of the various theoretical approaches is beyond the scope of this article. It is worthwhile to note that considerable progress has been made in the past few years in the calculation of the multiphonon absorption, which at first sight appears to be an extremely difficult higher order quantum mechanical calculation. Perhaps the simplest approach which yields relatively good agreement (at least at high temperatures) is the molecular Morse potential model of Maradudin and Mills (1973). While their solution is classical, it has been shown by Rosenstock (1973) that a quantum-mechanical solution can also be obtained and lattice dynamics introduced using the Debye approximation. Solutions of molecular models can also be obtained by use of diagram techniques although it becomes complicated in higher order. A more comprehensive quantum-mechanical approach in which the lattice dynamics is introduced using the central limit approximation has been carried out by Sparks and Sham (1973). It is important to note that there are some important differences among these various approaches which remain to be resolved. More extensive measurements of the frequency and temperature dependence of the intrinsic absorption should be helpful for comparison with theory.

4.2 Intrinsic and Impurity Absorption

Based upon an extrapolation procedure, an intrinsic absorption limit for KCl of about 0.00008 cm^{-1} is expected. The best starting material employed in this investigation had a room temperature absorption coefficient of 0.0002cm^{-1} where no attempt was made to subtract out the surface absorption. In this low range, slight differences in surface preparation can lead to relatively large differences in the absorption coefficient. Consequently, the value of 0.0002cm^{-1} represents an upper limit on the intrinsic absorption. If an assumption is made that the extrinsic and intrinsic components have different temperature dependences, then the observed temperature dependence curve might reflect this.

Inspection of this curve (Fig. 5) reveals that within the limit of accuracy of the measurements, the temperature dependence if monotonically increasing. This suggests that the absorption has a significant intrinsic component. More accurate measurements might have revealed an extrinsic component. In addition, measurements below room temperature might indicate a break in the curve similar to that observed with samples of poorer quality.

Measurements of the frequency dependence of the absorption should also provide an indication of the ratio of intrinsic to extrinsic absorption. Measurements of this nature on high purity samples are now being carried out at NRL using tunable lasers and using the spectral emissivity at NELC.

ACKNOWLEDGMENTS

The authors are grateful to J. R. Hardy, T. C. McGill, D. L. Mills, H. B. Rosenstock, and M. Sparks for stimulating discussions on the theoretical aspects. The authors thank R. Pastor of Hughes Research Laboratories for KCl samples and discussions concerning Reactive Atmosphere Processing, J. W. Davisson for development of chemical polishing methods, and P. H. Klein for crystal growth of KCl samples.

REFERENCES

Davisson, J. W., Hass, M., Klein, P. H., and Krulfeld, M., "Growth, Finishing, and Optical Absorption of Pure Potassium Chloride Single Crystals", Proc. 1973 Conference on High Power Infrared Laser Windows, edited by C. A. Pitha.

See also J. Phys. Chem. Solids (in press).

Harrington, J. A., and Hass, M., "Temperature Dependence of Multiphonon Absorption," Phys. Rev. Letters 31, 710.

Hass, M., and F. W. Patten, "High Energy Laser Windows," Semiannual Report No. 1, ARPA Order 2031, Naval Research Laboratory.

Maradudin, A. A., and Mills, D. L. (1973), "Temperature Dependence of the Absorption Coefficients of Alkali Halides in the Multiphonon Regime," Phys. Rev. Letters 31, 718.

Rosenstock, H. B. (1973), "Multiphonon Absorption Alkali Halides: Quantum Treatment of Morse Potential," Proc. 1973 Conference on High Power Infrared Laser Window Materials, edited by C. A. Pitha.

Sparks, M., and Sham, L. J., "Temperature Dependence of Multiphonon Infrared Absorption," Phys. Rev. Letters 31, 714.

TEMPERATURE DEPENDENCE OF THE ABSORPTION COEFFICIENT OF SOME WINDOW MATERIAL SAMPLES

D. L. STIERWALT
Electronic Materials Sciences Division
Naval Electronics Laboratory Center
San Diego, CA 92152

Abstract

Spectral emittance was measured from 3 to 20 microns on samples of sodium fluoride, sodium chloride and potassium chloride provided by the Naval Research Laboratory. Spectra were taken at 77, 196, and 373K for each sample. Absorption coefficients were calculated from sample thickness and emittance data. Curves of absorption coefficient versus wavelength at the three temperatures will be presented.

Infrared spectral emittance measurements have been made on a variety of window material samples at several temperatures from 77 to 373K. Absorption coefficient curves have been derived from the data. Some of the results will be presented here.

The emittance spectra were taken over the 3 to 20 micron region by a method described previously.[1,2,3] Figure 1 presents data on a sample of sodium fluoride approximately 23mm thick furnished by the Naval Research Laboratory. Measurement temperatures were 77, 196, 273, and 373K. At wavelengths longer than 10 microns, the temperature dependence of the absorption coefficient is about what one would expect from two-phonon emittance bands. At short wavelengths, the absorption appears to be anomalous, actually increasing with decreasing temperature. The data from 3.5 to 5.5 microns on the 373K curve is rather uncertain as the signal was close to the noise level.

Data on a sample of potassium chloride grown at NRL (KCl-301) is shown in Figure 2. Sample thickness was 45mm. Again we see the expected temperature dependence at long wavelengths and the inverted dependence at short wavelengths.

Similar behavior is exhibited by the zinc selenide sample of Figure 3. This specimen was approximately 21mm in thickness from a boule grown by Raytheon.

The sample compartment is evacuated by an ion pump during measurement. The 373K spectrum is run first, followed by successively lower temperature runs. The pressure

varies from about 10^{-5} Torr at 373K to about 2×10^{-8} Torr at 77K. This variation suggests the possibility that something is being cryopumped onto the sample, which could account for the increased emittance observed at the lower temperatures. The thin stainless steel sidewalls of the sample holder cool much more quickly than the sample, so that most of the cryodeposits should be collected there. Repeated spectra taken over a period of several hours do not change appreciably, indicating that if the sample surface is contaminated by cryopumping, it is not a continuous process

REFERENCES

1. D. L. Stierwalt, Conference on High Power Laser Window Materials, October 1972, Vol. 1, p. 319.
2. D. L. Stierwalt and R. F. Potter, Semiconductors and Semimetals, Vol. 3, Chapter 3, (1967).
3. D. L. Stierwalt, Appl. Opt. 5, 1911 (1966).

Temperature (°K) and Wavelength Dependence of Absorption:

Fig. 1 NaF

Fig. 2 KCl

Fig. 3 ZnSe

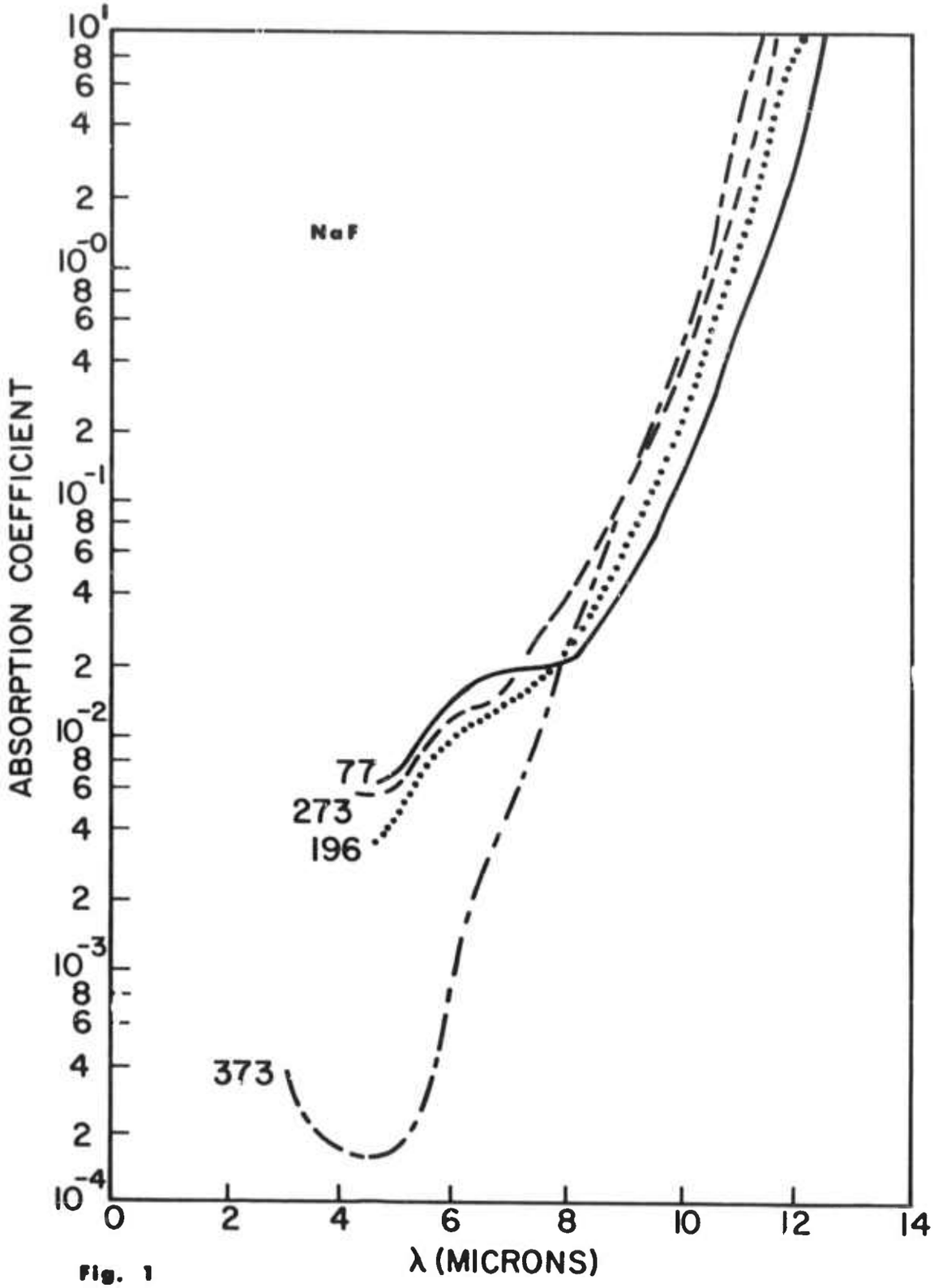
NaF
77
273
196
373
ABSORPTION COEFFICIENT
λ (MICRONS)
0
2
4
6
8
10
12
14

Fig. 1

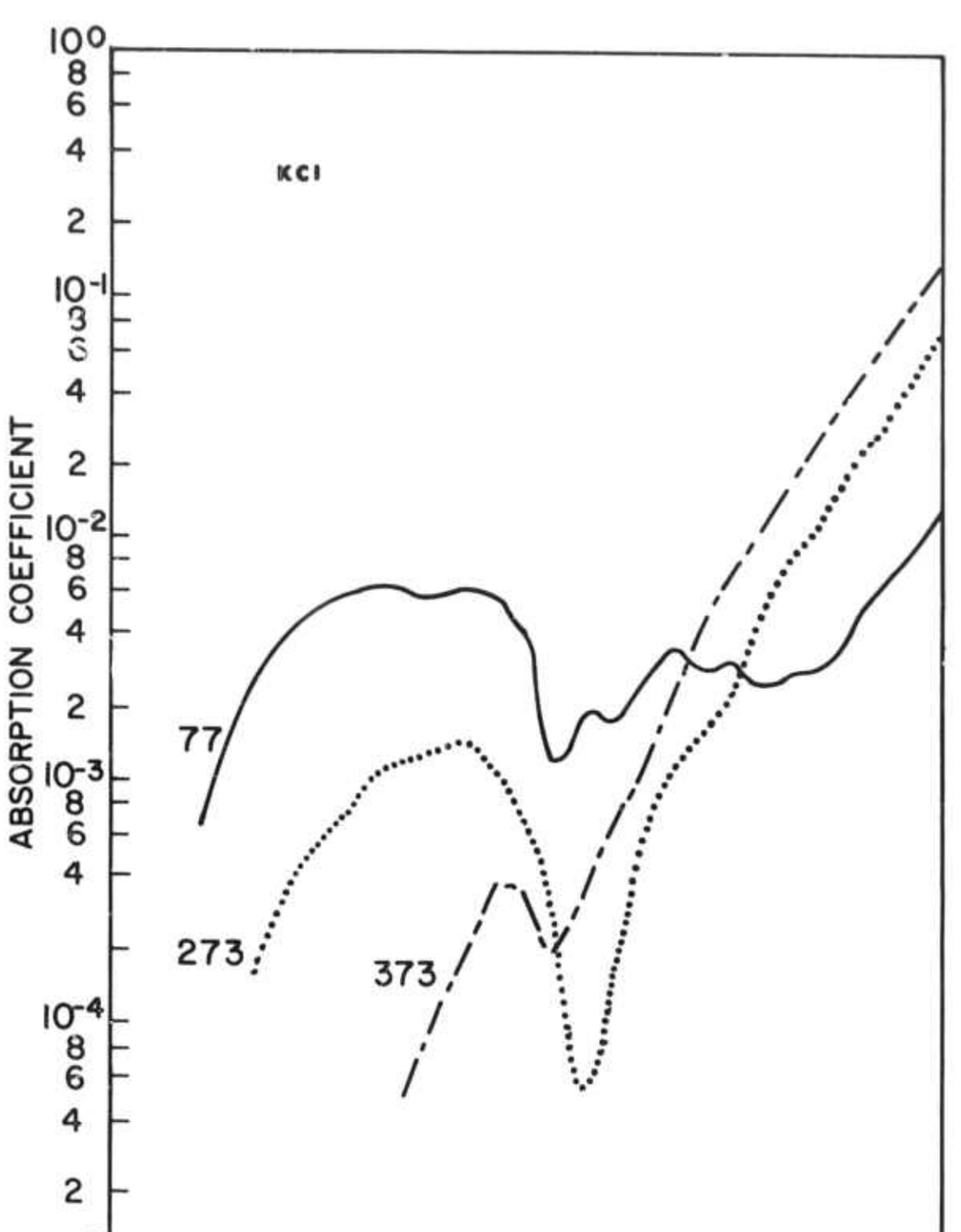
KCl
ABSORPTION COEFFICIENT
100
8
6
4
2
10-1
8
6
4
2
10-2
8
6
4
2
10-3
8
6
4
10-4
8
6
4
2
10-5
77
273
373
3
5
7
9
11
13
15
17
λ (MICRONS)

Fig. 2

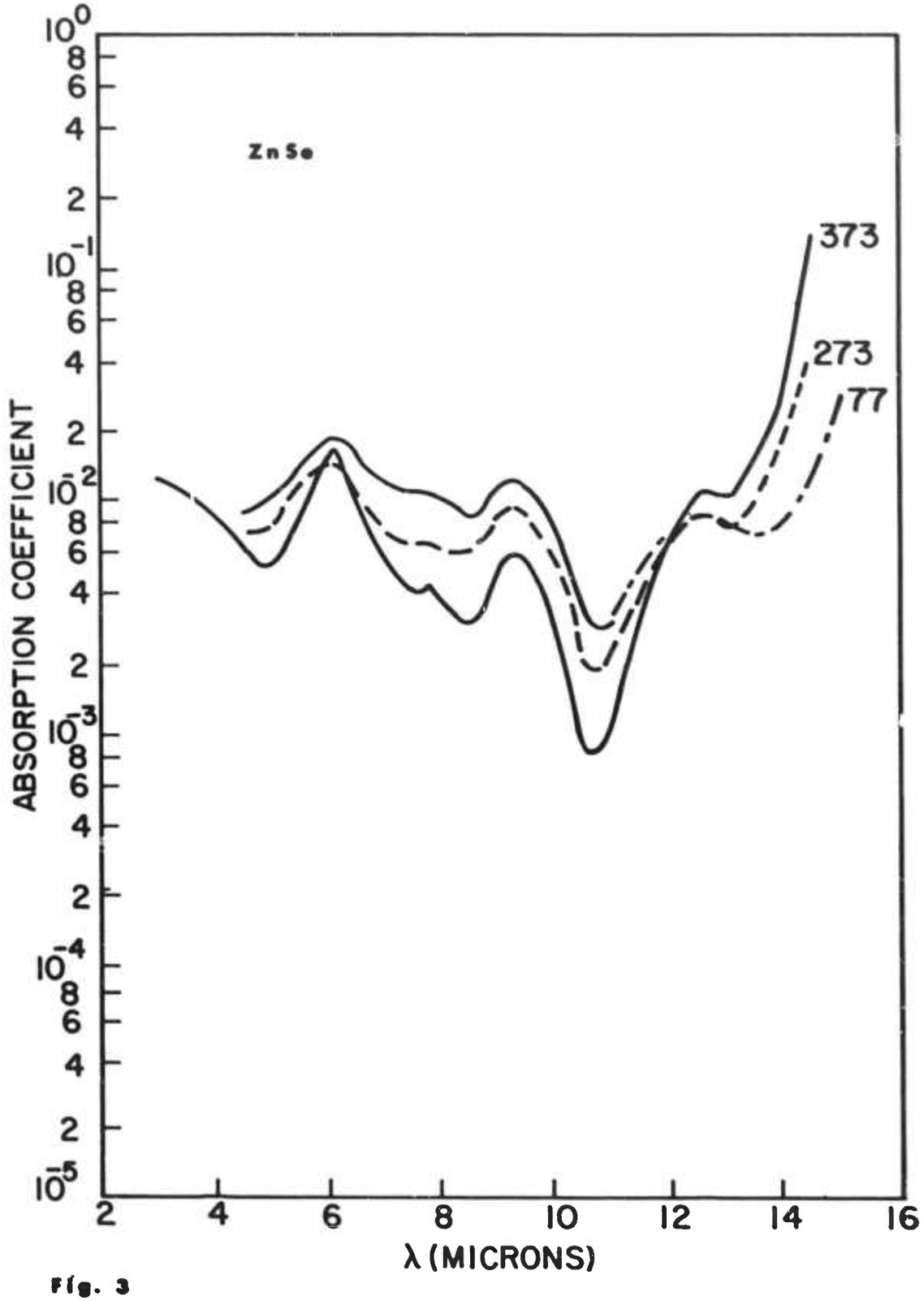
ZnSe
373
273
77
ABSORPTION COEFFICIENT
λ (MICRONS)
10^{0}
10^{-1}
10^{-2}
10^{-3}
10^{-4}
10^{-5}
2
4
6
8
10
12
14
16

Fig. 3

MULTIPHONON ABSORPTION IN ALKALI HALIDES: QUANTUM TREATMENT OF MORSE POTENTIAL

HERBERT B. ROSENSTOCK
U. S. Naval Research Laboratory
Washington, D. C. 20375

Abstract

With a view towards calculating the lattice absorption of solids, as a function of frequency and temperature, at frequencies much higher than that of the maximum lattice frequency, a quantum mechanical calculation is given of the absorption involving vibrational levels of a Morse potential that are not adjacent. The thermal average is then taken, and the nature of the solid simulated by a summation over a Debye spectrum. Results are compared with experimental results on the temperature dependence of absorption by alkali halides at 10.6 microns.

1. INTRODUCTION

Several workers have recently tried to calculate the absorption of insulating solids in regions of the infrared that would require the combined action of several phonons,[1,2,3,4,5,6] i.e. absorption of photons of energy 5-7 times that of the most energetic lattice phonon. Several of these papers[3,4] have either explicitly or by implication used the "Einstein" model of a solid: the solid is treated as an assembly of identical oscillators ("diatomic molecules"), independent but intrinsically anharmonic. In this model, the phonons that act together to provide the absorption all come from the same oscillator (or "diatomic molecule"). While it is realized that in the more usual model of a solid the phonons would come from different oscillators (where "oscillators" would mean the normal

modes of the lattice in the harmonic approximation, coupled to each other by the anharmonicity of the potentials), this "diatomic molecule" model is nonetheless used as an approximation. Each treatment obtained, either explicitly or by implication, a T^{n-1} dependence of the absorption at a given frequency on the temperature, with n the number of phonons required to achieve the process energetically. Most simply, this is shown to be just a consequence of the Boson occupation numbers obeyed by phonons.[1,5] Experimental results[7] have revealed a much weaker temperature dependence (T^0 to T^2 for absorption at 10.6 micron, where n for alkali halides would have to be at least 5-7). This has resulted in additional theoretical work to modify and elaborate earlier results[8,9].

One of the earlier approaches[4,9] provided a classical treatment of absorption by diatomic molecules for several choices of anharmonic interatomic potentials. Perhaps the most realistic of these potentials, the so-called "Morse Potential"[10] is, however, exactly soluble in quantum mechanics, and we therefore attempt here a quantum mechanical calculation of "multiphonon" absorption by a Morse potential, in the hope that this will be both more realistic particularly at low temperatures, and simpler and more transparent (in avoiding the complex statistical arguments that the classical approximation entails).*

We have put the word "multiphonon" in quotation marks in the last sentence, because the phonon concept does not really appear in our calculation. "Phonons" imply energy levels that are equally spaced, as arise in a structure that is treated as harmonic in the lowest approximation. In that lowest approximation, outside radiation can produce transitions between adjacent energy levels only ("one-phonon transitions"). Anharmonicity is in that approach treated by perturbation methods and allows transitions between energy levels that are not adjacent (" coupling between the phonons" or "multiphonon transitions"). By contrast, our potential is anharmonic from the beginning, and equally spaced energy levels, or "phonons" appear at no point. Radiation of the appropriate energy can then induce transitions between any pair of levels, and all are in

---

*More precisely, we use what is sometimes called "semiclassical radiation theory", in which the absorber is treated according to quantum mechanics, but the light as a Maxwellian electromagnetic wave. (See, e.g. L. I. Schiff, Quantum Mechanics, McGraw Hill, 1955, Ch. X). No use is made of second quantization techniques. The same approach has also been used with the Morse potential in Ref. 3.

general allowed; the main problem in essence is the calculation of the first order matrix elements for transitions induced by radiation between energy levels - not necessarily adjacent ones - that are separated by a specified energy gap. This was done long ago, and is set down in Section 2. The temperature dependence of the absorption is included by assigning Boltzman population factors to each level (Section 3), and integration over the lattice frequencies is done in Section 4. Numerical results and figures, giving the absorption as a function of both light frequency and temperatures are obtained in Section 5.

2. MORSE OSCILLATOR FORMULAS - TRANSITIONS TO NON-ADJACENT LEVELS

The empirical potential function

$$V(r) = D\left[1 - e^{-a(r-r_0)}\right]^2 \tag{1}$$

was introduced into molecular physics by Morse[10] for three reasons: because it reasonably represents the potential between two atoms an equilibrium distance r_0 apart [it is very large at $r = 0$; it has one minimum-zero-at $r = r_0$; and it approaches a finite value - the dissociation energy D - at $r = \infty$]; because its Schrödinger equation can be solved exactly; and because it leads to eigenvalues in agreement with experiments that measure the spacing of adjacent energy levels in molecules (i.e. one-phonon absorption experiments), at different temperatures. The eigenvalues are found to be finite in number,

$$E_n = \hbar\omega\left(n + \tfrac{1}{2}\right) - \left(\hbar^2\omega^2/4D\right)\left(n + \tfrac{1}{2}\right)^2 \tag{2}$$

for $n = 0, 1, \ldots, (k-1)/2$

with

$$\omega = a\left(2D/\mu\right)^{1/2}$$
$$k = \mathrm{Int}\left(4D/\hbar\omega\right) \tag{3}$$

μ the reduced mass, and $2\pi\hbar$ Planck's constant. Levels are thus seen to be approximately $\hbar\omega$ apart for small n, but very close together as the dissociation limit is approached. The wave functions are also known explicitly, but

will not be written down here. From them, one can compute[11] the probability for a transition from level m to level n caused by dipole radiation, and hence also the absorption coefficient per unit length in an assembly of Morse oscillators. This can be written[12]

$$\alpha(E_\ell, T, \omega) = \frac{4\pi^2 N}{\ell_\eta c n_o} \left(\frac{\mathcal{E}_{eff}}{\mathcal{E}_o}\right)^2 E_\ell f_\eta \tag{4}$$

with N the number of oscillators per unit volume, c the speed of light, n_o the index of refraction, η the polarization index, $(\mathcal{E}_{eff}/\mathcal{E}_o)$ the ratio between the effective local and the applied field, E_ℓ the energy of the incoming light,

$$f_\eta = |\langle m|P_\eta|n\rangle|^2 \delta(E_n - E_m - E_\ell) \tag{5}$$

and $P_\eta = e r_\eta$, summation being implied over all states m and n that satisfy the energy conservation requirement expressed by the delta function. Averaging over directions in a cubic lattice results in the subscript η being converted into a factor of (1/3). The matrix elements have been evaluated by Scholz[11] using generating functions methods. The result is

$$r_{mn}^2 = a^{-2}(n-m)^{-2} F_{mn} \tag{6}$$

with

$$F_{mn} = \frac{(k-1-2m)(k-1-2n)}{(k-1-m-n)^2} \frac{\binom{n}{m}}{\binom{k-1-m}{n-m}} \tag{7}$$

for $n > m$, and $r_{mn} = r_{nm}$ otherwise. $\binom{n}{m}$ denotes the usual binomial coefficient. Perhaps it is more appealing to write

$$n - m = \Delta \tag{8}$$

since for most applications Δ will be a small integer, while m, n themselves could be large integers at elevated temperatures. Then we have approximately

$$r_{mn}^2 = (a\Delta)^{-2}(m+1)(m+2)\ldots(m+\Delta)/k^\Delta. \qquad (m \ll k) \tag{9}$$

specifically

$$r^2_{m,m+1} = (m+1)/k a^2$$
$$r^2_{m,m+2} = (m+1)(m+2)/4k^3 a^2 \qquad (9')$$
$$r^2_{m,m+3} = (m+1)(m+2)(m+3)/9k^3 a^2$$

Thus transitions for any two levels Δ apart are possible, but with decreasing probability proportional to $(m/k)^{\Delta}$. In further work, we shall use the correct expression (6) rather than the approximate (9).

3. TEMPERATURE DEPENDENCE

Absorption of a photon of specified energy is possible if and only if the system is initially in a state that differs from a higher lying state by just that energy. The probability of being in such a state depends on the temperature, and consequently the probability of absorption does also. The absorption coefficient in (4) must therefore be weighted by the appropriate Boltzman factor

$$B_{m,m} = \left(e^{-\beta E_m} - e^{-\beta E_{m+\Delta}}\right)/Z \,. \qquad (10)$$

The normalizing constant

$$Z = \sum_{m} e^{-\beta E_m}$$

is usually called the partition function. As usual, we have written $\beta = (k_B T)^{-1}$ with k_B Boltzmann's constant. Two terms appear in the numerator because the probability of the inverse process (emission of a photon as the system goes from state $m + \Delta$ to state m) has to be subtracted from the absorption probability (as the system goes from m to $m + \Delta$) to give the net absorption probability; the matrix element r^2 is, as we have seen, the same for the two processes. Computation of the partition function is numerically the lengthiest part of the calculation. Depending on the values taken on by E_m and T, it can be done either directly or by the use of the Euler-MacLaurin summation formula. The details have recently been given elsewhere.[13]

4. SUM OVER LATTICE FREQUENCIES

If our interest were indeed in an ideal gas of one species of diatomic molecules, then the evaluation of (4) multiplied by (10) and summed over available states for photon energies $E_\ell = E_{m+\ell} - E_m$ would give our final result. But, in fact we are discussing the diatomic gas only as a model for an anharmonic solid. Restricting ourselves to one species of "molecule" therefore seems artificial; to be somewhat more realistic, we want to take account of the fact that the lattice frequencies span a continuous band from 0 to a fixed ω_{max}. A simple way of simulating this is to integrate the result of Section 3, which contains a frequency ω defined in terms of the parameters of the Morse potential by (3), over the known frequency spectrum of the lattice; the reader may think of this process as approximating the anharmonic lattice by a gas of independent diatomic anharmonic molecules not of one species but of many species, the basic frequencies of the molecules being chosen so as to match the known frequency distribution of the lattice.

Though plausible, it should be clear that this process is also somewhat artificial. The physical basis for integrating over a frequency distribution is the known theorem that the system of coupled harmonic oscillators can, by a canonical transformation, be decomposed into a system of uncoupled harmonic oscillators (each with its own frequency which is, in principle, known). This theorem does not apply to anharmonic oscillators; a system of coupled oscillators that are essentially anharmonic cannot be decomposed into a system of uncoupled oscillators. The "conventional" way to get around this and utilize the theorem after all is to begin with the harmonic approximation, make the decoupling transformation, and then consider the anharmonicity as a perturbation. That approach has been critized - cogently, we believe - as invalid for problems that are essentially, rather than just slightly, anharmonic[4,9]. This is therefore, not the approach of the present paper. We have instead chosen to start by approximating the system by an assembly of oscillators which are essentially anharmonic but, for simplicity, uncoupled. Consequently our subsequent integration over "lattice" frequencies, which derives from the other approximation, may seem to be a mixture of two different models. Nonetheless, an integration over the known lattice frequencies will surely provide more realism than restriction to a single frequency alone would.

To perform this integration over frequencies we use the Debye approximation

$$g(\omega) = \begin{cases} \omega^2 / 3\omega_{max}^3 & 0 < \omega < \omega_{max} \\ 0 & \text{otherwise} \end{cases} \qquad (11)$$

(Let us point out that the choice of this particularly simple frequency distribution is not necessary to carry the calculation further. A more realistic distribution would allow us to proceed almost as easily).

The fixed ω_{max} is chosen to fit the known reststrahl frequency. The dissociation energy D is held constant in the integration - a simplification that is justified by the fact that dissociation of a mode implies, in case of a solid, the breaking of some bond in the lattice; the energy required for this is the same for each mode, for every mode involves action of the very same bonds.

The absorption from such a "lattice" or "assembly" of oscillators is then

$$\alpha_{tot} = \int_0^{\omega_{max}} \frac{d\omega\ \omega^2}{3\omega_{max}^3} \sum_{\Delta=1}^{\cdot} \sum_{m=0} a(\omega, E_\ell, T) B_{m, m+\Delta} \qquad (12)$$

The integration is done after introducing $u = E_{m+\Delta} - E_m - E_\ell$, the argument of the delta function in (5), as the variable of integration. The final results appears in the form

$$\alpha_{tot} = C \bar{E}_\ell H P \qquad (13)$$

with

$$C = 2\pi^2 \xi / 137$$

$$H = k_{min} / \mu \omega_{max} n_0 a_0^3$$

$$a_0 =$$

$$P = \sum_{\Delta<1} \sum_{m=0} \Delta^{-3} B_{m+\Delta, m} F / (1 - 2Ax^*)$$

F and B given by (7) and (10), $\bar{E}_\ell = E_\ell / \hbar\omega_{max}$, $x = \omega/\omega_{max}$, $A = (2m+1+\Delta)/k_{min}$, x^* is the solution of the equation $E_{m+\Delta}(x) - E_m(x) - E_\ell = 0$ and E_m is given by (2). The final double sum is evaluated numerically.

5. NUMERICAL ESTIMATES

Our real interest is in alkali halide crystals, but the model is that of a gas of individual molecules. There is some question, therefore, whether we should evaluate our formulae with numbers appropriate to solid alkali halides, or to gaseous ones. We chose the latter. We find[15]

	KCl	NaCl
r_o (Angstroms)	2.76	2.36
$\hbar\omega_{max}$ (eV)	.0342	.0466
D (eV)	4.42	4.26
Δ (atomic masses)	18.4	13.8
T/T (°K)	400	422
a_o (Angstroms)	3.15	2.82
n_o	1.45	1.49

Here $\bar{T} = T/k_B\hbar\omega_{max}$ is a normalized temperature.

We also remember that at room temperature, $k_B T = \beta^{-1}$ is about .025 eV. The table shows that the spacing $\hbar\omega_{max}$ of low lying levels is about that energy, but that the dissociation energy D is larger by a factor of a hundred. Excitation of lower lying excited states is therefore quite probable for room temperature to perhaps 1000°K (the region for which data are available[7]), but excitation beyond the bound states is quite improbable at such temperatures. Thus, the assumption used in the preceeding section, viz. that $k_{min}\beta\hbar\omega_{max} \gg 1$ is quite appropriate.

We can now proceed to evaluate (13) numerically. Results are presented in two kinds of figures: Figure 1 gives absorption as a function of photon energy, for several fixed temperatures, for KCl. Figure 2, as a function of temperature, for several fixed energies for KCl and NaCl. Experimental results are also shown in Figure 2. Agreement is within

about a factor of 3, but the slope seems nearly correct.

At low temperatures, Figure 1 shows sharp discontinuities at points close to integer values of the phonon energy; this is a consequence of the need for a transition across n levels ($\Delta v = n$ "n-phonon transitions") when $\bar{E}_\ell$ is greater than n, whereas transitions across only n-1 levels which, by (9), are much more probable, suffice for $\bar{E}_\ell < n$. At higher temperatures, the higher probability of initial excited states, and the consequent availability of many more transitions that satisfy the energy conservation requirement, smooths out the discontinuities. It is interesting that similar structure appears in Ref. 9, though it is based on a wholly classical calculation.

The curves on the log-log scales of Figure 2 are nearly straight lines, suggesting that the power law, $\alpha \sim T^j$ does hold approximately; but j is appreciably smaller than n-1 (viz. about 4 for $\bar{E}_\ell = 7$, and about 2 for $\bar{E}_\ell = 3.36$, the normalized energy of a photon of wavelength 10.6 microns). Agreement with experiment is much better than should be expected from the crudity of our model.

6. SUMMARY

The formal calculations in this paper have been reported in greater detail recently.[13] The major differences between that and the present work are two; we have now dropped the restriction to "high" temperatures ($kT > \theta_{max}$) is no longer required), and the absorption coefficient has been calculated in an absolute scale (in cm^{-1}) rather than on an arbitrary scale. We have approximated the absorption of light by a solid in spectral regions well beyond that of the energy of lattice vibrations by a quantum mechanical calculation of a solvable anharmonic (Morse) potential. The virtue of the calculation is the complete avoidance of the harmonic approximation in this highly anharmonic situation; its weakness - describing a solid initially by an assembly of diatomic molecules - is somewhat ameliorated by performing a sum over the lattice frequencies (approximated by a Debye spectrum) in the end. At any fixed temperature, the absorption vs. frequency curves shows discontinuities at the frequencies at which additional "phonons" are needed to make the process allowable energetically; the discontinuities become less sharp as temperature goes up, and the envelop of the curve is always roughly exponential. At fixed frequen-

cies, on the other hand, the absorption vs. temperature curves approximately follow a power law, $\alpha \sim T^j$, with j appreciably smaller than the number of "phonons" involved in the process. Agreement with experiment is reasonably good.

7. ACKNOWLEDGMENTS

Part of this work was done at the Aspen Center for Physics, Aspen, Colorado. I am indebted to Dr. M. Hass, Dr. J. A. Harrington, Dr. A. R. Ruffa, Dr. B. M. Klein and Prof. E. Merzbacher for many discussions.

APPENDIX. ANALOGOUS EXPRESSIONS FOR THE HARMONIC OSCILLATOR

We should compare the matrix elements (6), (9) with the well known result for the harmonic oscillator,

$$r^2_{m,m+\Delta} = r^2_{m+\Delta,m} = \delta_{\Delta,1}\,(m+1)\Big/(2\mu(\omega/\hbar))$$

Since $k a^2$ turns out to be exactly $2\mu\omega/\hbar$ when the Morse potential (1) is expanded about its minimum to determine ω, this is in exact agreement with the first, but only the first of equations (9'); i.e. in the harmonic oscillator case, only transitions between adjacent states ("one phonon transitions") can be induced by electric dipole radiation, while with the Morse potential transitions between all levels are allowed (though with decreasing probability as the separation between levels increases). We also write down expressions for the matrix elements of powers of x (which are powers of $r^2 = x^2 + y^2 + z^2$):

$$\langle x^2\rangle^2 = (2\mu\omega/\hbar)^{-2}\left[(2m+1)\,\delta_{\Delta 0} + (m+1)(m+2)\,\delta_{\Delta 2}\right]$$

$$\langle x^3\rangle^2 = (2\mu\omega/\hbar)^{-3}\left[9(m+1)\,\delta_{\Delta 1} + (m+1)(m+2)(m+3)\,\delta_{\Delta 3}\right]$$

$$\langle x^4\rangle^2 = (2\mu\omega/\hbar)^{-4}\left[9(2m^2+2m+1)^2\,\delta_{\Delta 0} + (3+2m)(m+1)(m+2)\,\delta_{\Delta 2} + (m+1)(m+2)(m+3)(m+4)\,\delta_{\Delta 4}\right]$$

In absorption calculations, these matrix elements may arise in two ways: when higher order multipole radiation is considered, or when the harmonic oscillator potential is perturbed by cubic or quartic terms. The expressions are clearly reminescent of (9) but still have the property of vanishing beyond a certain - small - level separation. It is now clear that the rigorous vanishing of most of the matrix elements is an artifact introduced by beginning with the harmonic oscillator potential, which is not a natural start if one intends to deal with high lying levels, with anharmonicity that is large rather than a perturbation, or with high temperatures. The Morse potential, in which anharmonicity is appears ab initio rather than as a perturbation, is a potential which is not only more natural but also likely to provide a better basis as a starting point.

It is also instructive to compare our partition function with the one for the harmonic oscillator. For the harmonic oscillator, the E_n are equally spaced, viz. given by $\hbar\omega\left(n+\frac{1}{2}\right)$, i.e. by (2) without the quadratic term. Z sums exactly to $\left(1-e^{-\beta\hbar\omega}\right)^{-1}$ and in the limit of small β (high temperature) thus approaches $\left(\beta\hbar\omega\right)^{-1}$ just as for the "Morse" case. However, more importantly, the sum must also be taken in the numerator of (10), for energy conservation is, precisely because of the equal spacing of energy levels, satisfied for all levels if it is satisfied for any one m. Since $r^2_{m,m+\Delta}$ goes as m^{Δ}, the sum over m will go as $\left(1-e^{-\beta\hbar\omega}\right)^{-\Delta}$, or $\left(\beta\hbar\omega\right)^{-\Delta}$ in the small-β limit. Dividing by Z then shows that the absorption goes as $\left(\beta\hbar\omega\right)^{-\Delta+1} \sim T^{\Delta-1}$ in the high temperature limit. This is the "usual" result obtained in many more complicated methods but basically analogous to this one, and is quite different from the present result which gives a weaker dependence (see figures).

This $T^{\Delta-1}$ dependence of the absorption coefficient in any approximation that begins with the harmonic oscillator can also be derived in a way that is, or at least appears to be, different, by using in the language of second quantization; let us verbalize this briefly. What used to be called the nth excited state of the harmonic oscillator is now referred to as the presence of n phonons; the quantity $N^{(a)} = \sum_n E_n e^{-\beta E_n}/Z = \left[e^{-\beta E^{(a)}}-1\right]^{-1}$, previously the mean energy of the system at temperature T, is now viewed as the phonon occupation number of system (a) (quantitatively correctly, if phonons obey Bose-Einstein statistics). If i systems of harmonic oscillators are then caused to interact by some perturbation (such as an incoming photon), the probability of that

process is[14]

$$[1+N^{(a)}]\{1+N^{(b)}\}\ldots[1+N^{(i)}] - N^{(a)}N^{(b)}\quad N^{(i)}.$$

The leading term, which involves i-1 of the N's, will again go as T^{i-1} for high temperature, where i, analogous to Δ in the preceding paragraph, is the "number of phonons".

REFERENCES

1. Hardy, J.R., and Agrawal, B.S. (1973) Appl. Phys. Letters 22, 236.
2. Sparks, M., and Sham, L.J. (1973) Solid State Communications 11, 1451.
3. McGill, T.C., Hellwarth, R.W., Mangir, M., and Winston, H.V., J. Phys. Chem. Solids, in Print.
4. Mills, D.L., and Maradudin, A.A. (1973) Phys. Rev. B8, 1617.
5. Rosenstock, H.B. (1973) J. Appl. Phys. 44, 4473.
6. Namjoshi, K.V., and Mitra, S.S. Phys. Rev., in print.
7. Harrington, J.A., and Hass, M. (1973) Phys. Rev. Letters 31, 710.
8. Sparks, M., and Sham, L.J. (1973) Phys. Rev. Letters 31, 714.
9. Maradudin, A.A., and Mills, D.L. (1973) Phys. Rev. Letters 31, 718.
10. Morse, P.M. (1929) Phys. Rev. 34, 57.
11. Scholz, K. (1932) Z. Physik 78, 751.
12. Henry, C.H., Schnatterly, S.E., and Slichter, C.P. (1965) Phys. Rev. 137, A583.
13. Rosenstock, H.B. Physical Review, in print.
14. Dirac, P.A.M. Principles of Quantum Mechanics (3rd edition, Oxford 1947, Sec. 61).
15. American Institute of Physics Handbook (3rd edition, McGraw-Hill 1972, pages 7-176, 7-178 6-83, 9-8).
16. Harrington, J.A., and Hass, M. Proceedings of this corference. I am grateful to these authors for the early use of their data.

FIGURE CAPTIONS

Fig. 1. Absorption vs photon energy at various temperatures, for KCl. In each case the phonon energy is scaled to the "fundamental" or "reststrahl" mode (see table in Sec. 5).

Fig. 2. Absorption vs temperature for various phonon energies, for KCl and NaCl. Data points from reference 16.

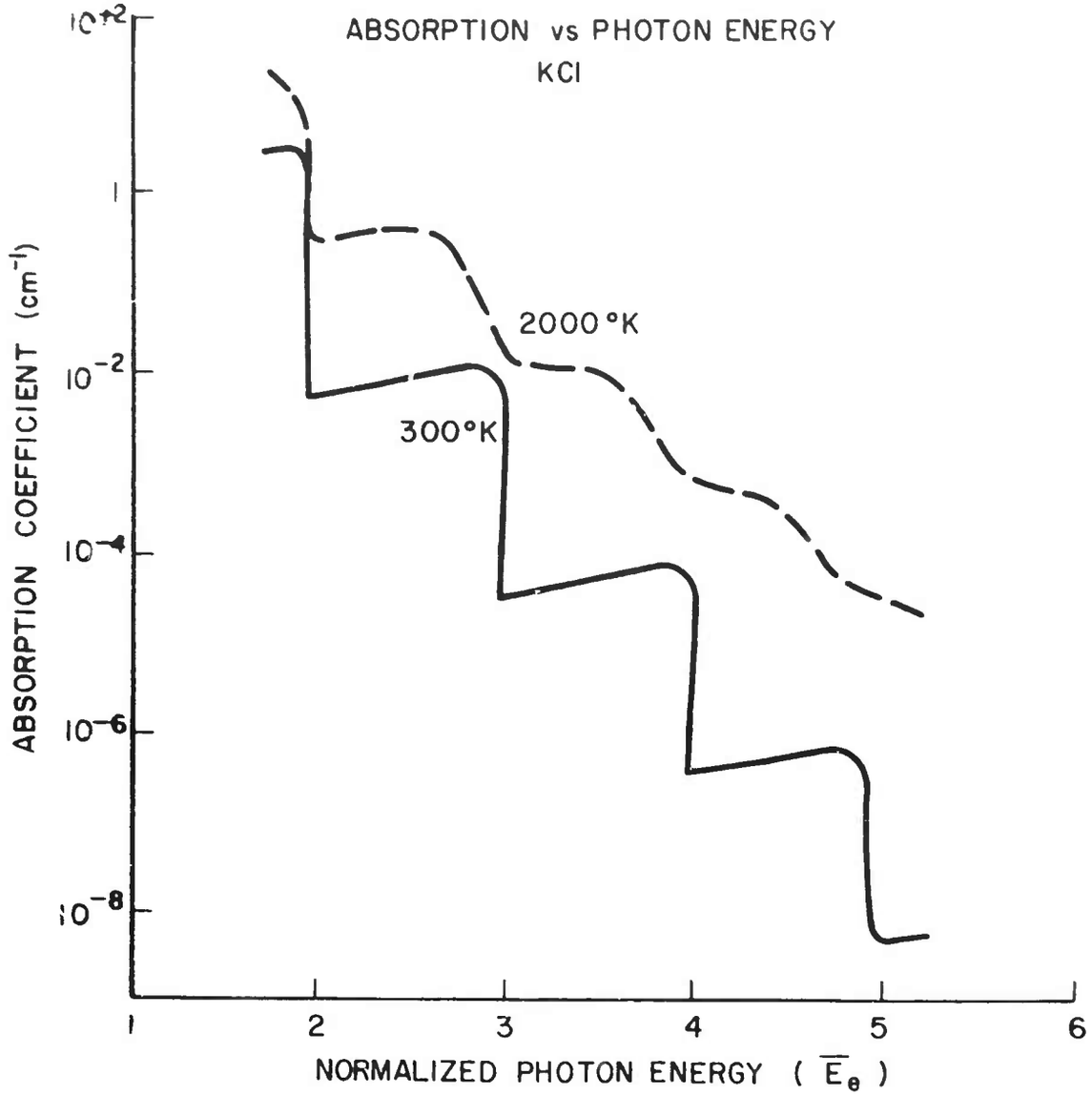
ABSORPTION vs PHOTON ENERGY
KCl
2000°K
300°K
ABSORPTION COEFFICIENT (cm⁻¹)
10⁺²
1
10⁻²
10⁻⁴
10⁻⁶
10⁻⁸
1
2
3
4
5
6
NORMALIZED PHOTON ENERGY ($\overline{E}_e$)

FIG. 1

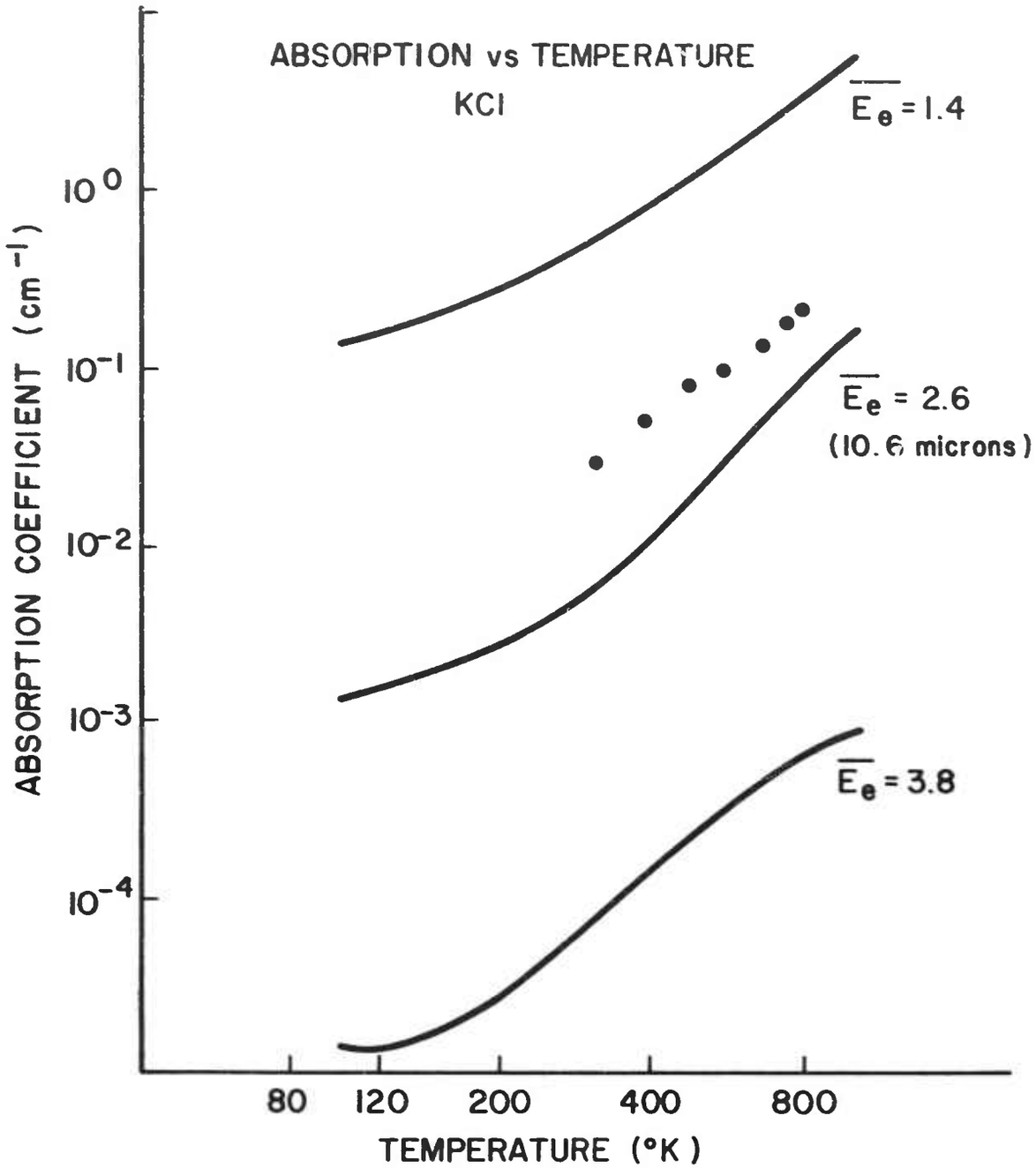
ABSORPTION vs TEMPERATURE
KCl
$\overline{E_e}$ = 1.4
$\overline{E_e}$ = 2.6
(10.6 microns)
$\overline{E_e}$ = 3.8
ABSORPTION COEFFICIENT (cm^{-1})
10^0
10^{-1}
10^{-2}
10^{-3}
10^{-4}
80
120
200
400
800
TEMPERATURE (°K)

FIG. 2

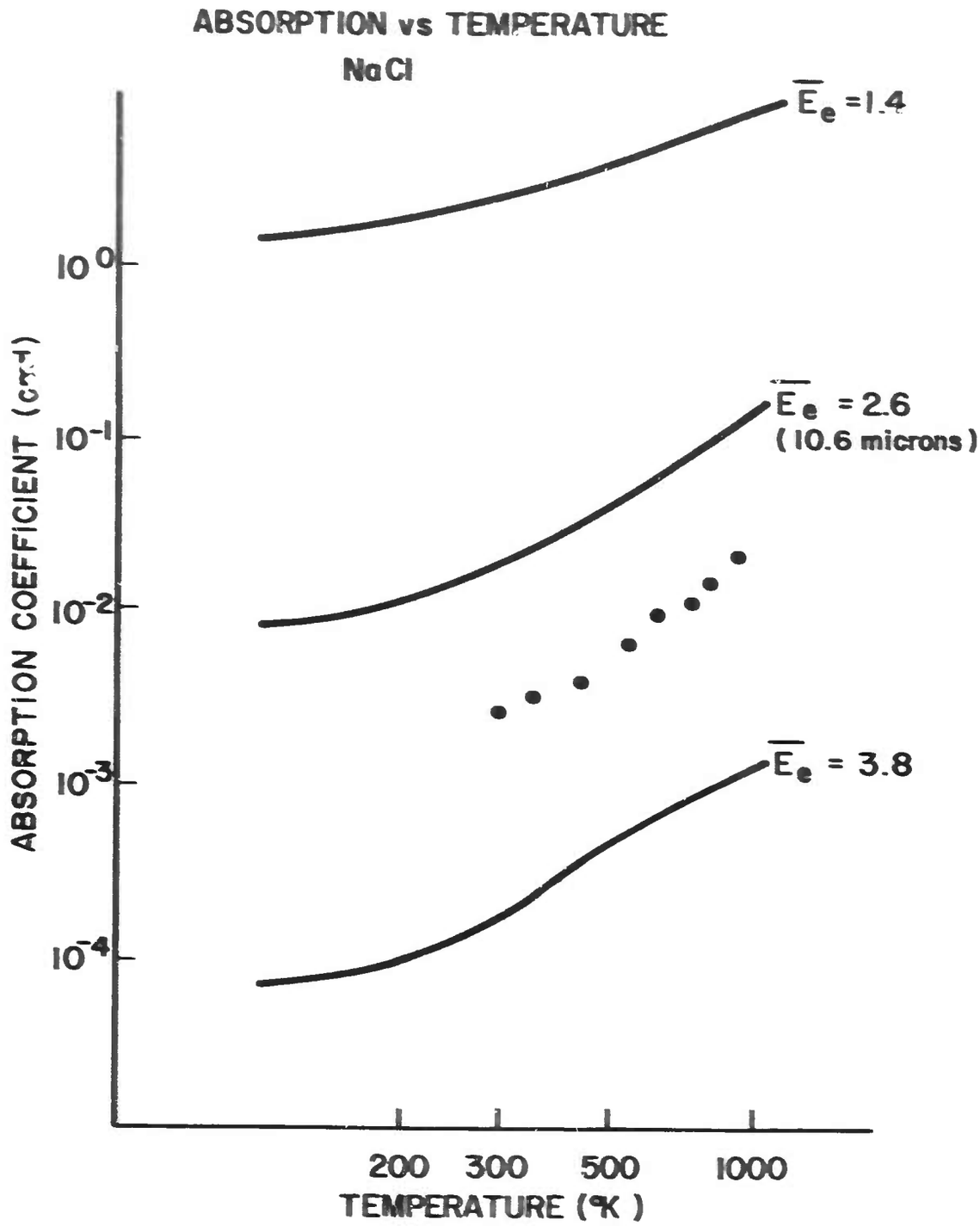
ABSORPTION vs TEMPERATURE
NaCl
$\overline{E}_e$ =1.4
$\overline{E}_e$ = 2.6
(10.6 microns)
$\overline{E}_e$ = 3.8
ABSORPTION COEFFICIENT (cm-1)
10 0
10-1
10-2
10-3
10-4
200 300 500 1000
TEMPERATURE (°K)

FIG. 2 (Cont'd)

APPENDIX

This appendix was prepared to discuss yield phenomena and present some further data on fracture energy. The recent Hyannis Conference on Laser Window Materials indicated some concern about yield stress measurements which are discussed here. Further, if dislocations are a factor in degrading optical behavior, then the microyield stress, discussed below, may be an important design parameter.

Yield Stress Behavior

The macroscopic yield stress, i.e., the point of the onset of gross plastic flow, does not represent the beginning of dislocation motion, but a transition in dislocation behavior. Several types of yield stress determination give similar but slightly different magnitudes of this stress ($\leq$20% total difference in stress level); however, results are consistent within each method. The proportional limit (used in this work, Fig. 1) is the first detectable macroscopic departure from linear elastic behavior, and the lowest value of yield strength. Somewhat higher, but possibly less variable, results are obtained by a linear offset method (intersection of stress-strain curve with a line parallel to the elastic region but offset by x strain, see Grant et al (1973)), while an intermediate value is obtained by the use of the intersection of a linear extrapolation of the plastic curve with the elastic portion of the stress-strain diagram (see Readey et al (1973)).

In single crystals and highly textured polycrystalline materials, the yield stress, independent of the method used to define it, depends on the angles between the stress axis and (1) the slip plane normal (θ) and (2) the slip direction (Φ). Such variations are normalized to a resolved shear stress on the slip system for a given body by the use of the Schmid factor ($\cos\theta \cos\Phi$). For {101}<101> slip in the same KCl crystal having a constant resolved shear stress, the observed yield stress decreases in the order of <111>, <110> to <100> for the applied stress axis; thus yield stresses are compared by noting the stress axis or the resolved shear stress. Other factors affect the yield stress as well, such as surface perfection, strain rate, environment, etc.

As noted, macroscopic yield occurs well after the onset of dislocation motion and represents substantial motion and multiplication of dislocations in the form of slip band propagation. This precursor dislocation activity below the macro-yield stress causes a small amount of nonlinear stress-strain behavior, and its detection is very dependent on the sensitivity of the strain measurement (generally $<10^{-3}$). This region between true elastic behavior and macroscopic yield is known as the microyield regime.

Some of the approximations of the microyield stress are when the stress ~1/2 the macroyield stress (e.g., as observed by Imura (1972) in Fe-3% Si crystals and Stokes (1962) in MgO crystals), or that the microplastic strain is $<10^{-3}$ (Lawley, 1968) or less than the elastic strain in this region (Brown, 1968). Using Fig. 1, where the highest macroyield stress is ~5500 psi and assuming the macroyield stress is less than half this, the elastic strain, thus microplastic strain within these two stresses, is $<7\text{x}10^{-4}$. Small microplastic strains are further suggested by the agreement between the Young's modulus based on the data points and from elastic moduli calculations ($5.73\text{x}10^{6}$ psi). However, the effect on microplastic strain on the optical behavior of a window may be important. If so, this could apply to any window material, as Lawley (1968) suggests the true microyield stress may be in the range of 10^{-5} times the shear modulus (e.g., <20 psi for KCl crystals). At present, it is not clear whether alloyed and/or polycrystalline KCl would behave any different.

A limited study of microyield in the KCl window materials will be carried out in a second test facility having strain measurement apparatus with a sensitivity of $2\text{x}10^{-5}$ to establish microyield effects. This would give an improvement of two orders of magnitude in sensitivity over that in the presently used apparatus and allow stress-strain behavior to be studied well within the microyield region.

Fracture Energy

The fracture strength of a window material is a function of the energy required to create two new crack surfaces by nucleation or growth of inherent flaws under stress. The importance of fracture energy in limiting crack propagation was shown by Loomis and Satio (1973) in observation of cleavage crack catastropic propagation

through a single crystal KCl window (low fracture energy), while cracks propagated short distances and then stopped in polycrystalline KCl (high fracture energy) during laser irradiation. Similar results have been shown by Becher and Rice (1973), e.g., Fig. 2 where most of the cracks propagated sporadically, advancing only when sufficient slip developed within the strain fields at the crack tip.

Observations by Blaszuk (1974) further emphasize the role of slip and slow crack growth in failure of KCl crystal windows under 10.6μm irradiation. He is using <100> and <111> uncoated windows, 4-1/4 to 5-1/4" diameter by 5/8 to 1-1/4" thick, on a commercial 10 KW laser with 30 torr inside pressure and a 2-3/4" diameter beam. Under crossed polars, plastic strain fields within these windows are observed to increase in intensity and the window bows inward when subjected to these low beam intensities and mild operating pressures. Though some windows can be repolished and reused, experience has shown that after a few reconditionings, window life is questionable because of increased probability of slow crack growth during subsequent irradiation. This slow crack growth can even occur after the window is removed and placed in a dessicator. Cracks initiate on the unpolished periphery of the windows where stress analysis shows the tensile stress to be enhanced by a factor of 2-3. Optical polishing of the periphery is underway and radial compression to limit the edge cracking is being considered. Under these present conditions, the operating life-time is generally limited by plastic deformation and slow crack growth, but one <100> KCl crystal window, 1" thick, has been operating in excess of 50 hours.

The above observations indicate that plastic deformation by $\{\bar{1}01\}\langle 101\rangle$ slip which intersects the (100) crack planes assists crack growth. Such effects have been directly observed in our fracture energy tests, showing that limiting plastic deformation should increase the fracture energy to propagate cracks. Our most recent studies have shown that the cleavage fracture energy (γ_f) of single crystal and polycrystalline KCl increases with the resolved shear stress for slip as follows:

$$\gamma_f = A\tau_y$$

where $A = 2\times10^{-5}$cm for KCl and $\sim 1\times10^{-5}$cm for NaCl.

Further fracture energy studies will incorporate KCl crystals and forgings having a wider range of yield stresses to determine if fracture topography (i.e., crack deflection at grain boundaries) enhances the polycrystalline fracture energy. Also, the effects of residual processing strains on the fracture energy of polycrystalline KCl will be investigated.

REFERENCES

1. Becher, P. F. and Rice, R. W. (1973), Semi-Annual Report No. 2, ARPA Order 2031, Naval Research Laboratory.

2. Blaszuk, P (1974), Private Communication.

3. Brown, N. (1968), pp. 45-73 in Microplasticity, C. J. McMahon, Jr. (ed.), Interscience Publishers, New York.

4. Grant, N. J. (1973), Annual Technical Report, ARPA Order 2055, Massachusetts Institute of Technology.

5. Imura, T. (1972), pp. 104-133 in Electron Microscopy and Structure of Materials, G. Thomas, R. M. Fulrath, and R. M. Fisher (eds.), University of California Press, Berkeley.

6. Lawley, A. (1968), pp. 75-90 in Microplasticity, C. J. McMahon, Jr. (ed.), Interscience Publishers, New York.

7. Loomis, J. S. and Saito, T. T. (1973), to be published in Proceedings of Third Annual High Power Infrared Laser Window Materials, C. A. Pitha (ed.), AFCRL, Bedford, Mass.

8. Readey, D., Newberg, R. and Miles, P. (1973), ibid.

9. Stokes, R. J. (1962), Trans. AIME 224:1227.

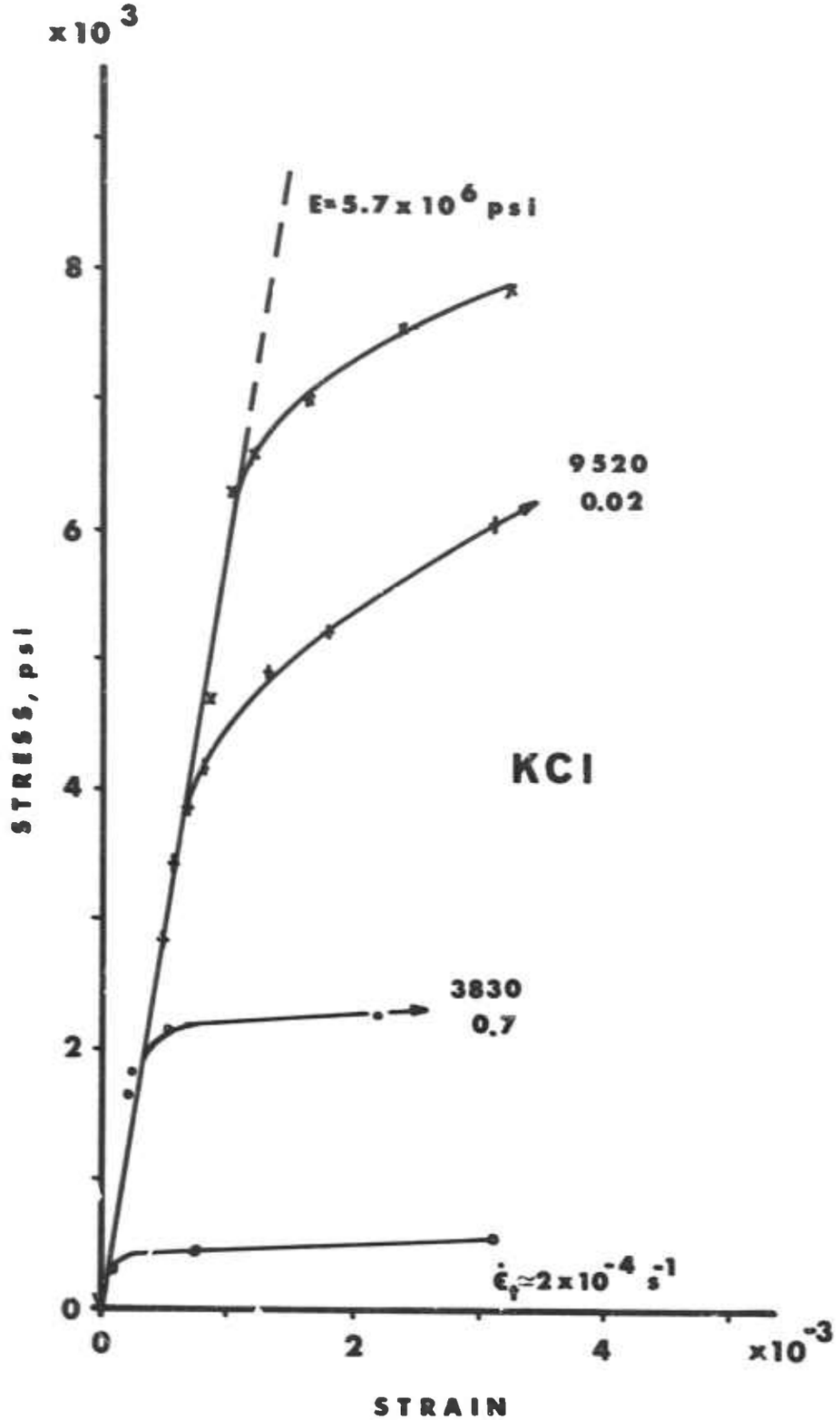

Figure 1. Stress-Strain Behavior of KCl at 20°C.

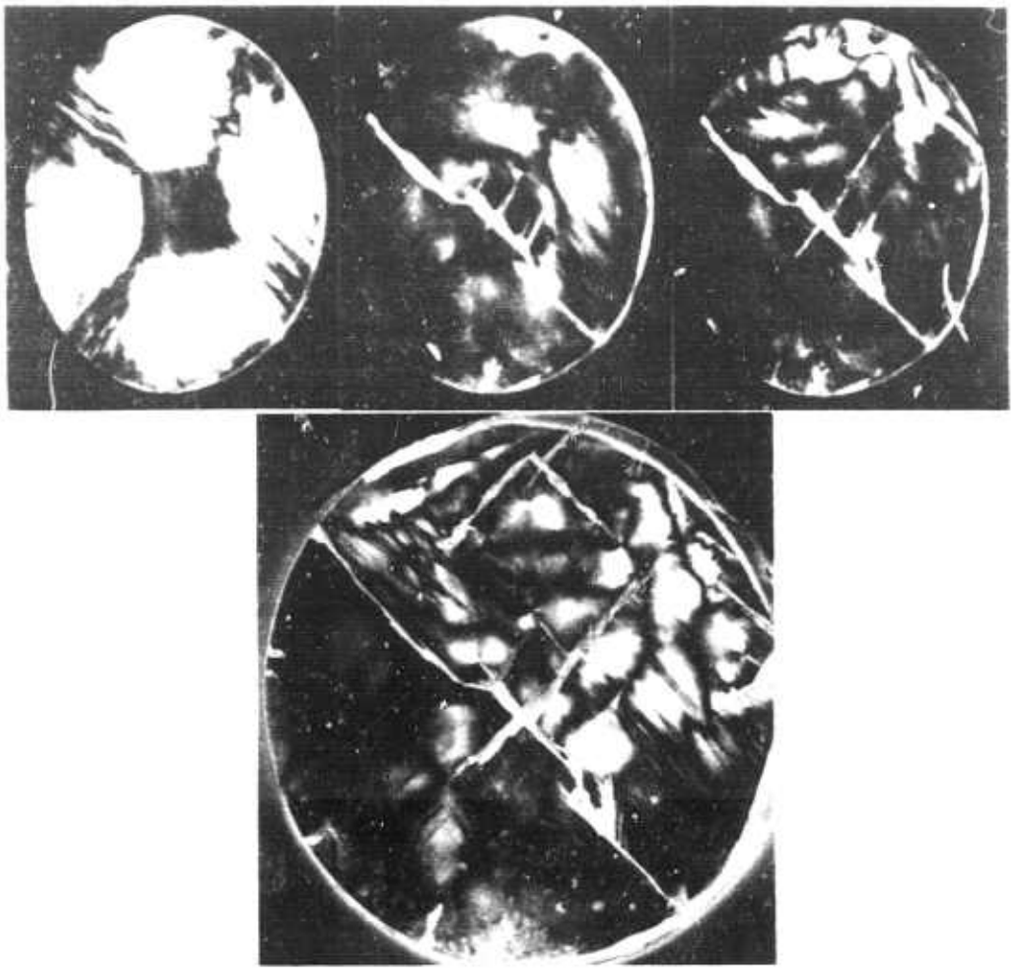

Figure 2. Strain Patterns and Crack Propagation in KCl During Irradiation.

Upper figures show the strain fields developed and slow crack growth with increasing irradiation time (left to right). Note position of cracks at center lying in NE direction. Lower figure shows details of cracks and associated crack tip plastic strain fields.